SURFACE OZONE MODELLING for Kiev city (in the frame of the program **Eurotrac-2**)

A.V. Shavrina(1), Veles A.A.(1), Dyachuk V.A.(2),, Nochvay V.(3), O.B. Blum(4), Sosonkin M.G(1), Eremenko N.A.(1), Mikulskaya I.A.(5), Below V.M. (5)

(1)Main Astronomical Observatory of National Academy of Sciences, Ukraine,

(2) Institute of Hydrometeorology, Ukraine

(3) National University of Kyiv-Mogyla Academy (now- in MAUP)

(4) Botanical Garden of National Academy of Sciences, Ukraine

(5) International Scientific-Educational Center of the Information Technologies and Systems of National Academy of Sciences of Ukraine

ABSTRACT

The modelling of ozone episode of August 2000 for Kiev city is discussed. For simulation of ozone concentrations, the Prognostic Meteorological Model (PMM) and Urban Airshed Model (UAM-V) (SAI of USA) are used. The episode of enhanced ozone concentrations for 17-21 August 2000 from monitoring data of Kiev Botanic Garden was selected for modelling. A rather high ozone concentrations exceeding Ukrainian and European limit values were predicted for north-east part of city.

The results of model calculations show an importance of more detailed temporal modulation of emission data, in particular hourly NO, NO_2 and VOC data, and the necessity of taking into account night time heterogeneous chemistry.

INTRODUCTION

It is common knowledge that the stratospheric ozone layer (in the upper atmosphere) is very important for sustaining life on Earth - the ozone layer protects life on Earth from the harmful and damaging ultraviolet solar radiation.

Ozone in the lower atmosphere, or troposphere, acts as a pollutant but is also an important greenhouse gas. Ozone is not emitted directly by any natural source. However, tropospheric ozone is formed under high ultraviolet radiation flux conditions from natural and anthropogenic emissions of nitrogen oxides (NOx) and volatile organic compounds (VOCs).

While in European region the monitoring of surface ozone is carried out at more than 1700 site stations, in Ukraine the ozone concentrations were not measured before a recent time. Only from 1996 the permanent automatic registrations of ozone concentrations were organized in National Botanic Garden (Kiev) with the help of ultraviolet ozone analyzer TECO 49. The same analyzer was installed at the Main Astronomical Observatory of National Academy of Sciences in summer 2006. Preliminary results of analysis of O3 measured data, air quality state stations measurements and first steps of modeling permit to do some main conclusions relative to formation of surface ozone in Kiev city.

Why ground-based ozone monitoring and modelling are important?

- Now satellite observations are available for total ozone and tropospheric columns, nevertheless ground based monitoring and modelling is needed to validate and complement space-based measurements and to clarify local/regional specific sources and sinks of ozone and each greenhouse gas. These data can help to study the dynamical behavior of air pollution from space and ground-based observations and to check compliance to the pollutants transport models.

- They will also serve to development of an environmental policy, greenhouse gases policy in particular, in a local and regional scale.
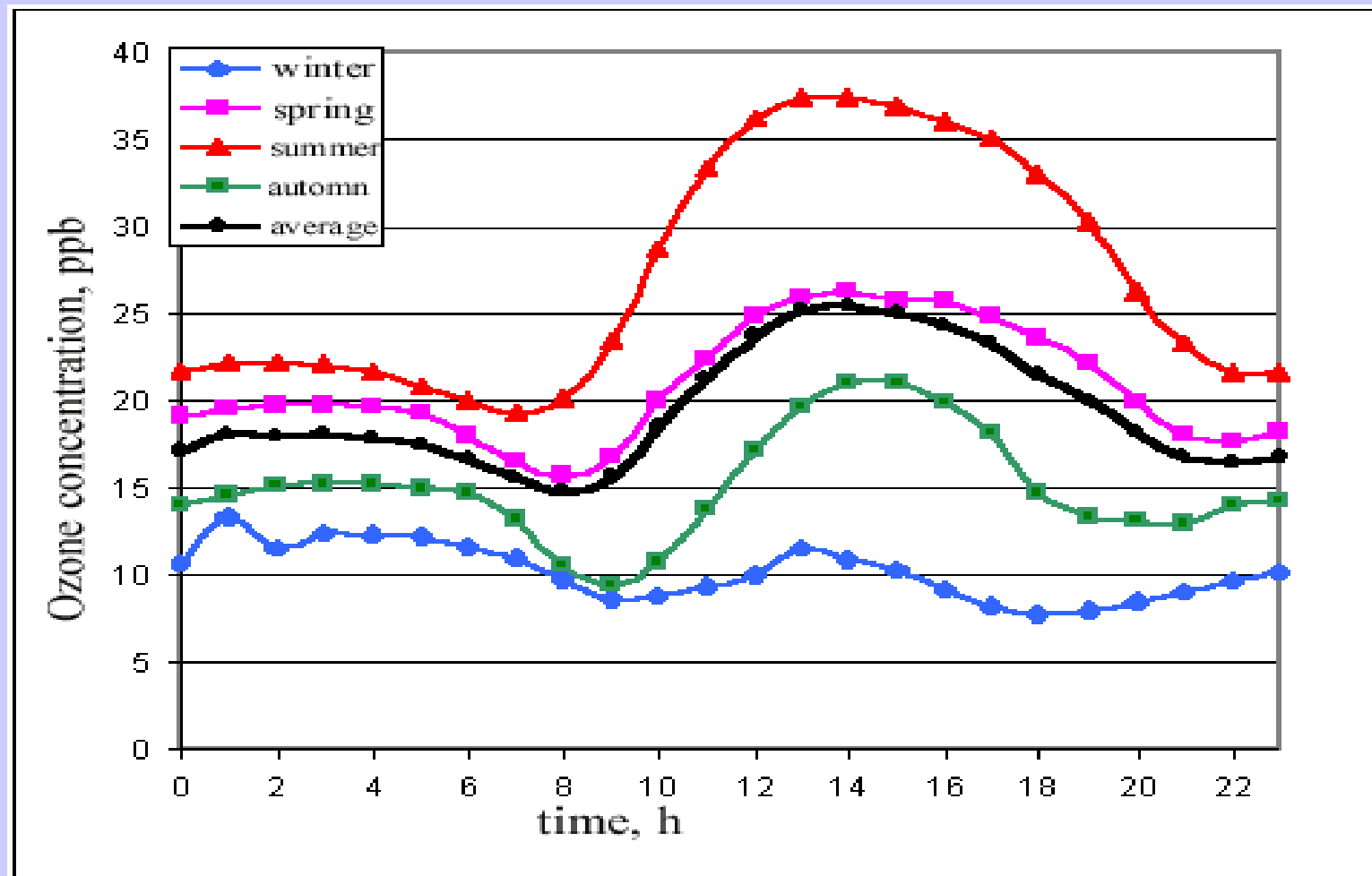
Figure 1. Average for year 2000/01 and averaged for seasons hourly ozone concentrations, ppb

The analysis of surface ozone measurements **in National Botanic Garden (Kiev) with the help of ultraviolet ozone analyzer TECO 49** for 2000 year (Sosonkin et al. 2002) permit to do some main conclusions relative to surface ozone levels in Kiev city. The average annual concentrations of surface ozone are near to 19.5 parts per billion (ppb) , which exceed average daily limited concentration for Ukraine, 30 mkg m(-3) or 15 ppb, as it is given in the Guide (Rukovodstvo po kontrolyu zagryazneniya atmosfery. Leningrad: Hydrometizdat, 1979, 448 p. (Atmosphere pollution control's quide))

Seasonal variations of ozone concentration are presented in Fig.1, maximum of this value was observed in July-August, minimum - in winter.

Meteorology and wind field

The synoptic situation at 18-21 August was characterized by predominance of small-gradient high pressure field with a mild cold arctic front, slowly moving above Ukraine area. Near the earth surface, it was dominant the west wind of 1-3 m/sec, at altitudes up to 1000 m - south and south-west winds (2-15 m/sec), the temperature was changed from 18-20º C up to 30-35º C around-the-clock, the temperature inversion with intensity of 0.5-2.01º C was formed during each night. This type of synoptic processes was favorable for significant accumulation of ozone precursors, primary from area sources (traffic predominantly), and subsequent intensive ozone production in city's area under weak mechanism of natural self-cleaning of the atmosphere, that was satisfied by the results of primary calculations.
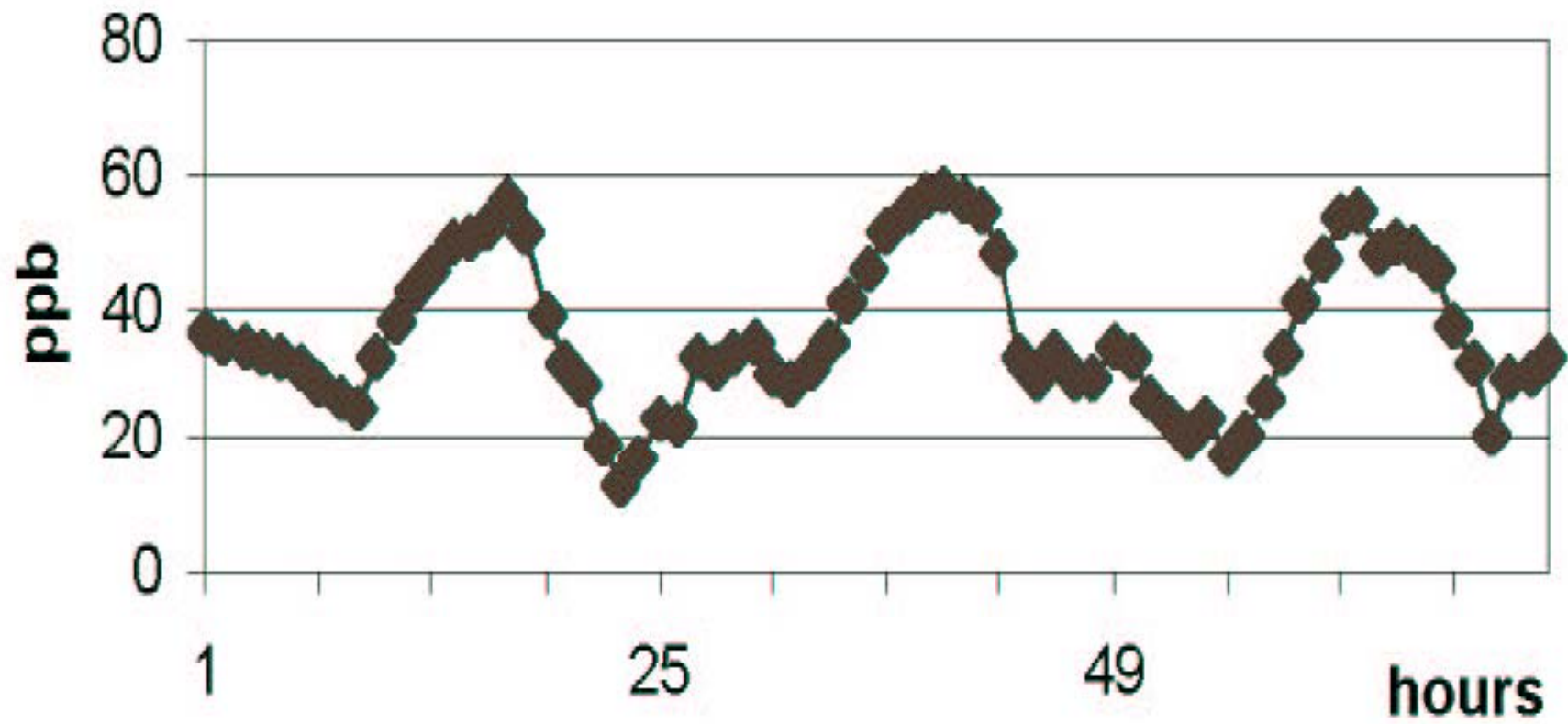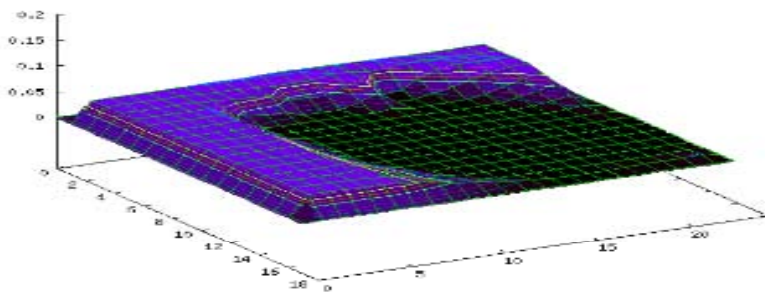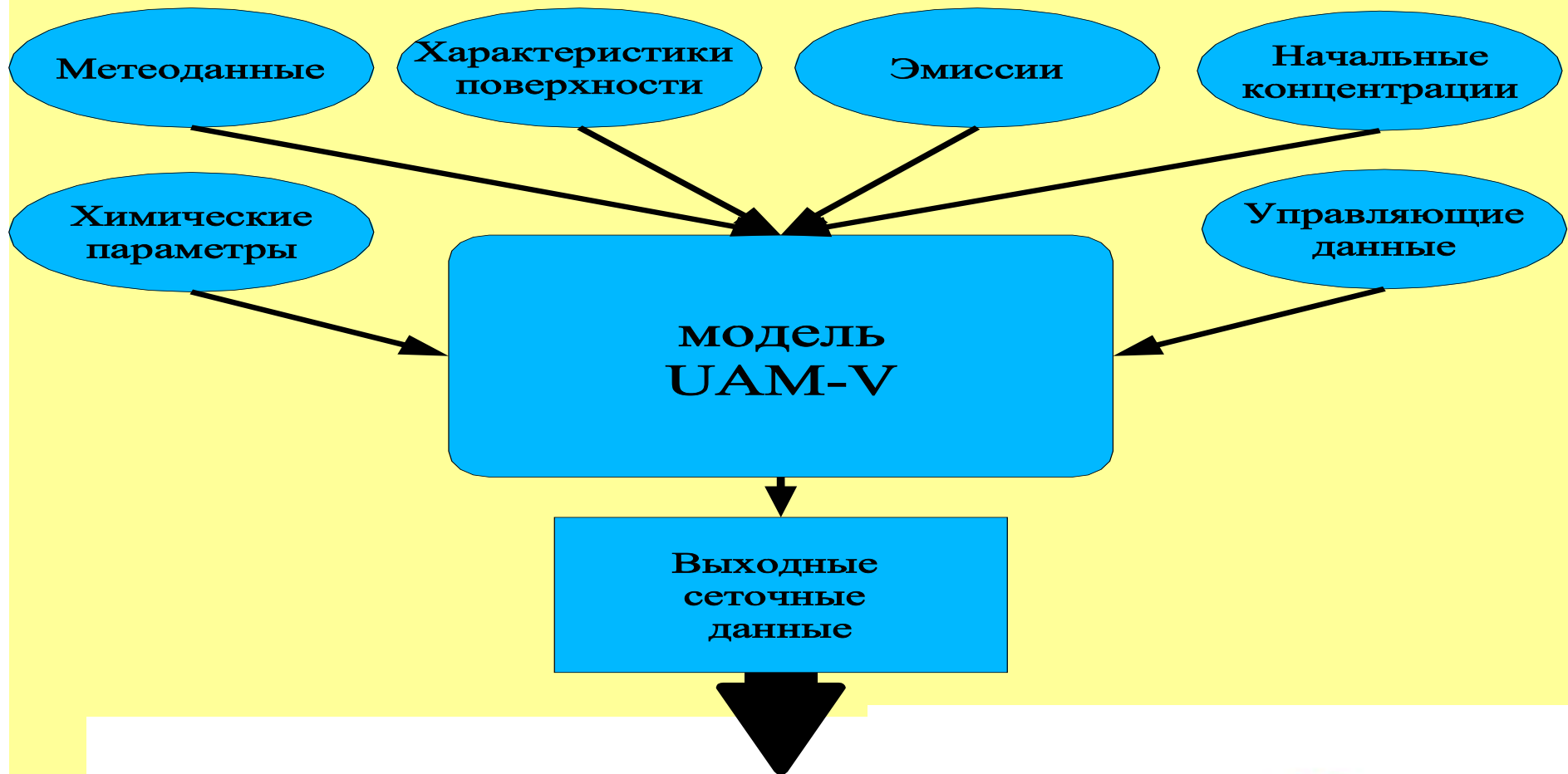
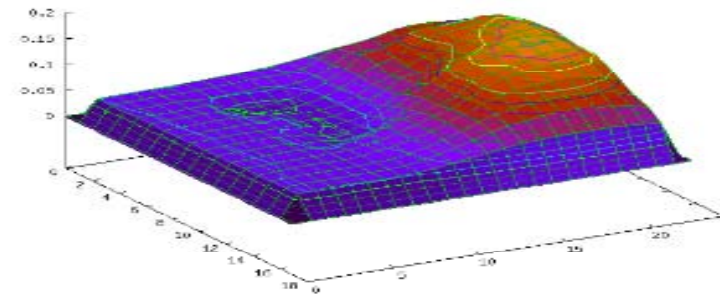Figure 3: Ozone time series for entire episode (19-21 Aug 2000).

The Prognostic Meteorological Model SAIMM

The Prognostic Meteorological Model (PMM SAIMM) was used as preprocessor for meteorological data needed for modelling of ozone concentrations. The coarse grid for PMM was consisted of 18x18 cells of 4x4 km and corresponded to most part of Kiev region. The measurements of temperature, pressure, humidity and wind parameters - velocities and directions of wind on ground level at 6 weather stations of Kiev region and balloon measurements (up to 10 km of altitude) at one station (Kiev), twice a day, were used for wind and temperature fields simulation.

In the process of simulation with PMM the background fields were reconstructed, adjusting wind fields to local topography. Finally PMM model provides 3D wind and temperature fields as well as turbulence parameters for input to Urban Airshed Model UAM-V.

2. TECHNICAL FORMULATION

The variable-grid Urban Airshed Model (UAM-V) system is a three-dimensional grid (Eulerian) model designed to calculate the concentrations of both inert and chemically reactive pollutants by simulating the physical and chemical processes in the atmosphere that affect pollutant concentrations. The basis for the UAM-V model is the atmospheric diffusion equation (also called the species continuity or advection/diffusion equation). This equation represents a mass balance in which all of the relevant emissions, transport, diffusion, chemical reactions, and removal processes are expressed in mathematical terms as follows:

$$\frac{\partial c_i}{\partial t} + \frac{\partial(uc_i)}{\partial x} + \frac{\partial(vc_i)}{\partial y} + \frac{\partial(wc_i)}{\partial z} = \frac{\partial}{\partial x}\left(K_X\frac{\partial c_i}{\partial x}\right) + \frac{\partial}{\partial y}\left(K_Y\frac{\partial c_i}{\partial y}\right) + \frac{\partial}{\partial z}\left(K_V\frac{\partial c_i}{\partial z}\right)$$

Time Dependence   Advection   Turbulent Diffusion

$$+ \quad R_i \quad + \quad S_i \quad + \quad D_i \quad + \quad W_i$$

Chemical Reaction   Emissions   Dry Deposition   Wet Deposition

where

c_i	=	concentration of pollutant i, a function of space (x,y,z) and time (t)
u,v,w	=	horizontal and vertical wind speed components
K_X, K_Y	=	horizontal turbulent diffusion coefficients
K_V	=	vertical turbulent exchange coefficients
R_i	=	net rate of production of pollutant i by chemical reactions
S_i	=	emission rate of pollutant i
D_i	=	net rate of change of pollutant i due to surface uptake processes
W_i	=	net rate of change of pollutant i due to wet deposition processes

Input Data Required by the UAM-V Model

The UAM-V derived pollutant concentrations are calculated from the emissions, advection, and dispersion of precursors and the formation and deposition of pollutants within every grid cell of the modeling domain. To adequately replicate the full three-dimensional structure of the atmosphere during an ozone episode, the UAM-V program requires an hourly and day-specific database for input preparation. Several preprocessing steps to translate raw emissions, meteorological, air quality, and grid-specific data are required the develop final UAM-V input files.

The new features of the UAM-V model necessitate the provision of more extensive input data compared to the earlier version. Observed air quality data are used to evaluate model predictions. These data may also be used to estimate the initial concentrations and boundary conditions for ozone, NOx , and volatile organic compounds (VOC). The UAM-V model is usually used to simulate a multiday episode, and the simulation is started during the early morning hours one to three days before the start of episode. Use of start-up days limits the influence of the initial concentrations (which are not well-known) on the simulation of the primary episode days.

Emissions inventory

Evaluation of emission rates due to various sources of pollution for Kiev city in August 2000 were carried out according to statistical emission data for separate industrial plants. Among the point-source emission species we took into account the next ones: nitrogen oxides, saturated and unsaturated hydrocarbons, and formaldehyde. From the anthropogenic and biogenic sources distributed on grid cells, the emissions of carbon oxide and main components of Volatile Organic Compounds (VOC), 22 compounds altogether, were estimated additionally. Emissions of specified species from traffic were estimated according relative composition of exhaust gas of automobile cars.

Pollution by stationary sources is due to more than 700 plants of different branch of industry, on which there are 24 thousands of organized emission points of atmosphere pollution. The most contribution in city's atmosphere pollution from industry is due to combined heat and power (CHP) plants, emissions from which in year 2000 are composed 19,386 ton (60% of pollutions from stationary sources). For today the road traffic in Kiev, like to number of other towns of Ukraine, is one of main sources of atmosphere pollution. Our estimates for NO_x and VOC due traffic are 3,348 and 10,460 ton accordingly. Total VOC amount was split into individual compounds[7] and than lumped into the emission classes needed by the photochemical mechanism CB-IV-TOX implemented in the UAM-V model.

Emission sources were grouped as point and area ones on city's domain. Among point sources, 16 high stationary sources were selected for emission modelling. Their emission volume in the summer 2000 put together more than 80% of industrial pollution. For each point source, the next stack parameters were included as input data for modelling: stack height, diameter of stack, stack exit velocity and exit temperature for gas-air mixture.

The other 20% of stationary point sources were taken into account together with mobile sources as area emission sources. The city's domain was presented as a cell grid of 17 x 15, with size of each cell of 2 x 2 km. Emission from each cell was estimated on the base of traffic volume on roads within each cell and district averaged emissions of stationary sources, which were not accounted as point sources.

The UAM-V species continuity equation using nested grids is solved as follows:

1. Emissions are injected into the coarse grid.

2. Transport/diffusion/deposition are integrated on the coarse grid for one coarse-grid advective (driving) time step.

3. For each fine grid:

(a) If necessary, coarse-grid input data are interpolated to the fine grid.

(b) A driving time step is defined for the fine grid that is an integral subdivision of the coarse-grid time step.

(c) Emissions are injected.

(d) Transport/diffusion/deposition are integrated.

(e) Chemistry calculations are carried out.

Emission rates

Evaluation of **emission rates** due various sources of pollution for Kiev city in August 2000 were carried out according to statistical emission data for separate industrial plants from **Minicipal Report.**

Among the point- source emission species it was taken into account the next ones: nitrogen oxides, saturated and unsaturated hydrocarbons, and formaldehyde. From the anthropogenic and biogenic sources distributed on grid cells, the emissions of carbon oxide and main components of Volatile Organic Compounds (VOC), 22 compounds altogether, were estimated additionally.

Emissions of specified species from traffic (area sources) were estimated according relative composition of exhaust gas of automobile car cited in the book of **Isidorov, 2001.** Total VOC amount was split into individual compounds and than lumped into the emission classes needed by the photochemical mechanism **CB-IV-TOX implemented in the UAM-V model.**

Dnieper river
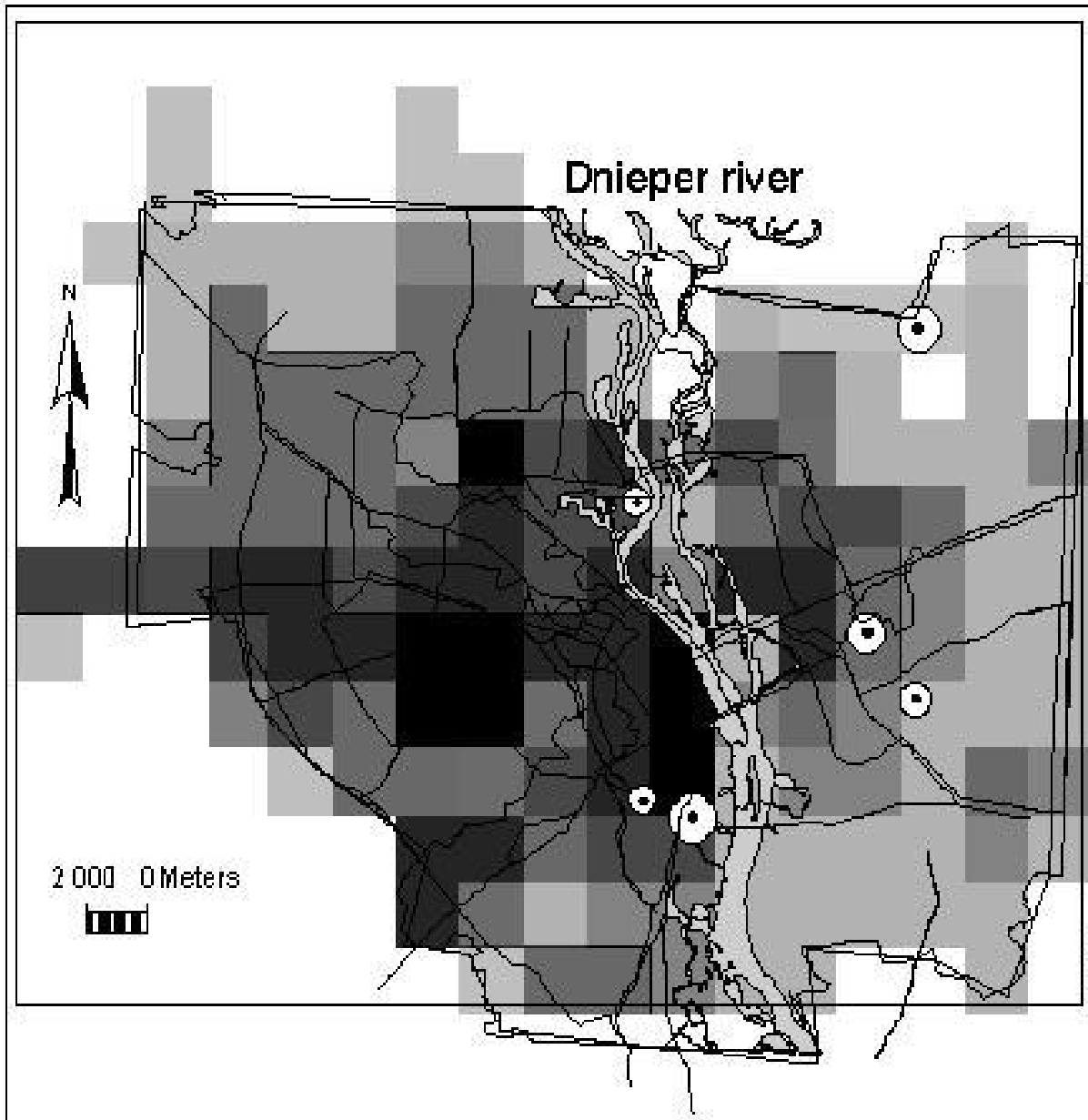
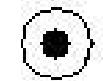Emission from cells, g hour-1

Value

0 - 780

780,01 - 25 468

25 469 - 38 422

38 423 - 50 397

50 398 - 88 938

66 837 - 82 695

82 696 - 104 760

104 770 - 129 600

2 000   0 Meters

Heat Power Plants emissions
(emission proportional dimension)

uam-v modelling

Two days simulation of ozone episode for 19-20 August 2000 were performed scaling emission data averaged daily and hourly on the basis of annual volumes. In the Figure 5 we show the comparison of calculated with UAM-V ozone concentrations and data of measurements in National Botanic Garden for 19-20 August 2000. One can see on Figure 3 that O_3 concentrations show non-linear variation depending on average hourly NO_x emission data (curves 2,3). The comparison of ozone concentrations with measurements shows the necessity of temporal modulation of VOC and NO_x emissions taking into account diurnal traffic intensity and specific weekday variations (curve 4). It is known, that the ratio of NO and NO_x is very badly determined both for industrial and traffic emissions and can change of factor up to 10^7), therefore we scaled their emission data separately for each species.
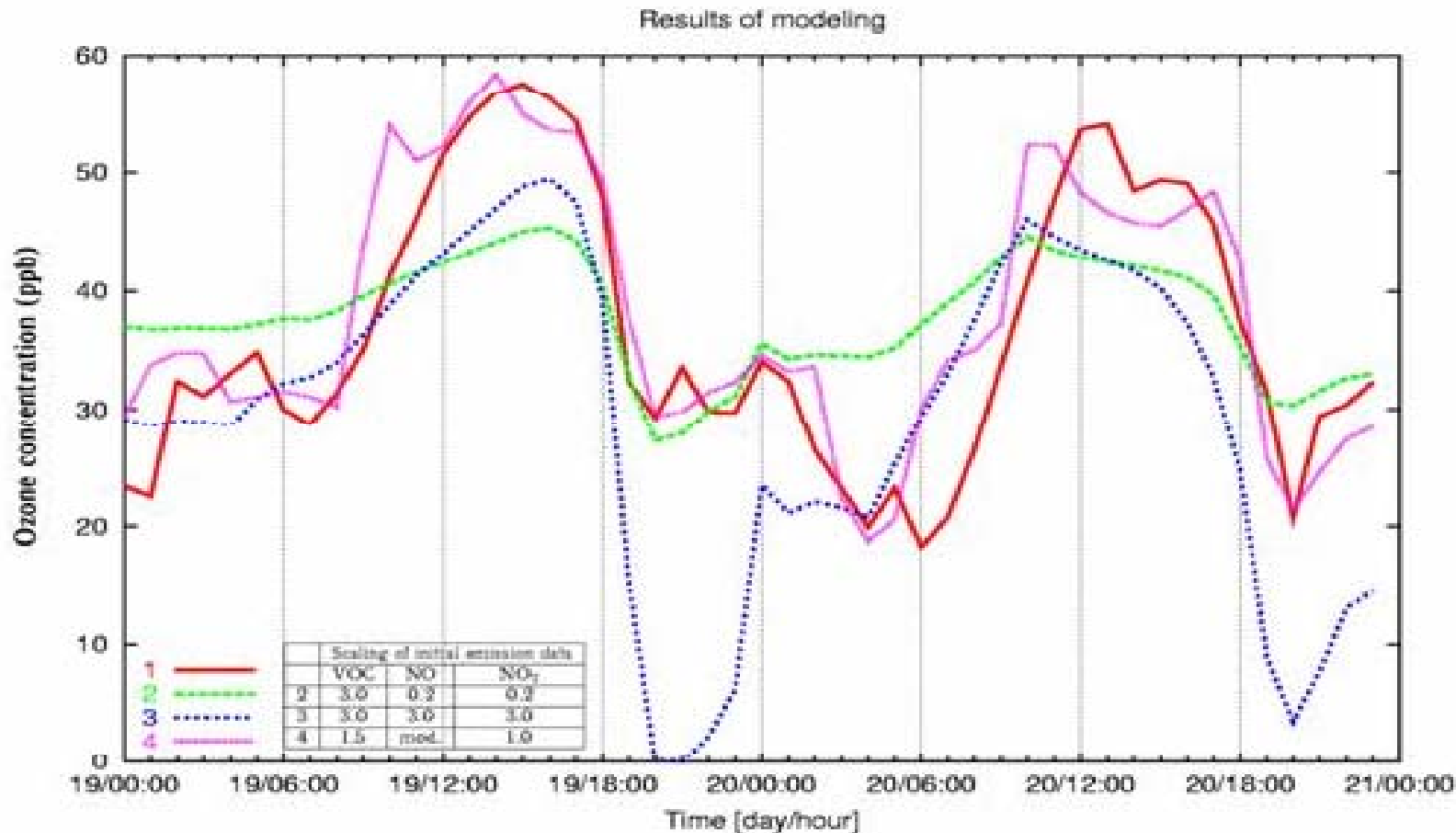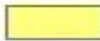
Figure 5: The comparison of measured (red line) and calculated (lines 2-4) O3 concentrations for Aug 19-20, 2000. Lines 2 and 3 are scaled hourly average emissions, line 4 is modulated ones according diurnal traffic motion.
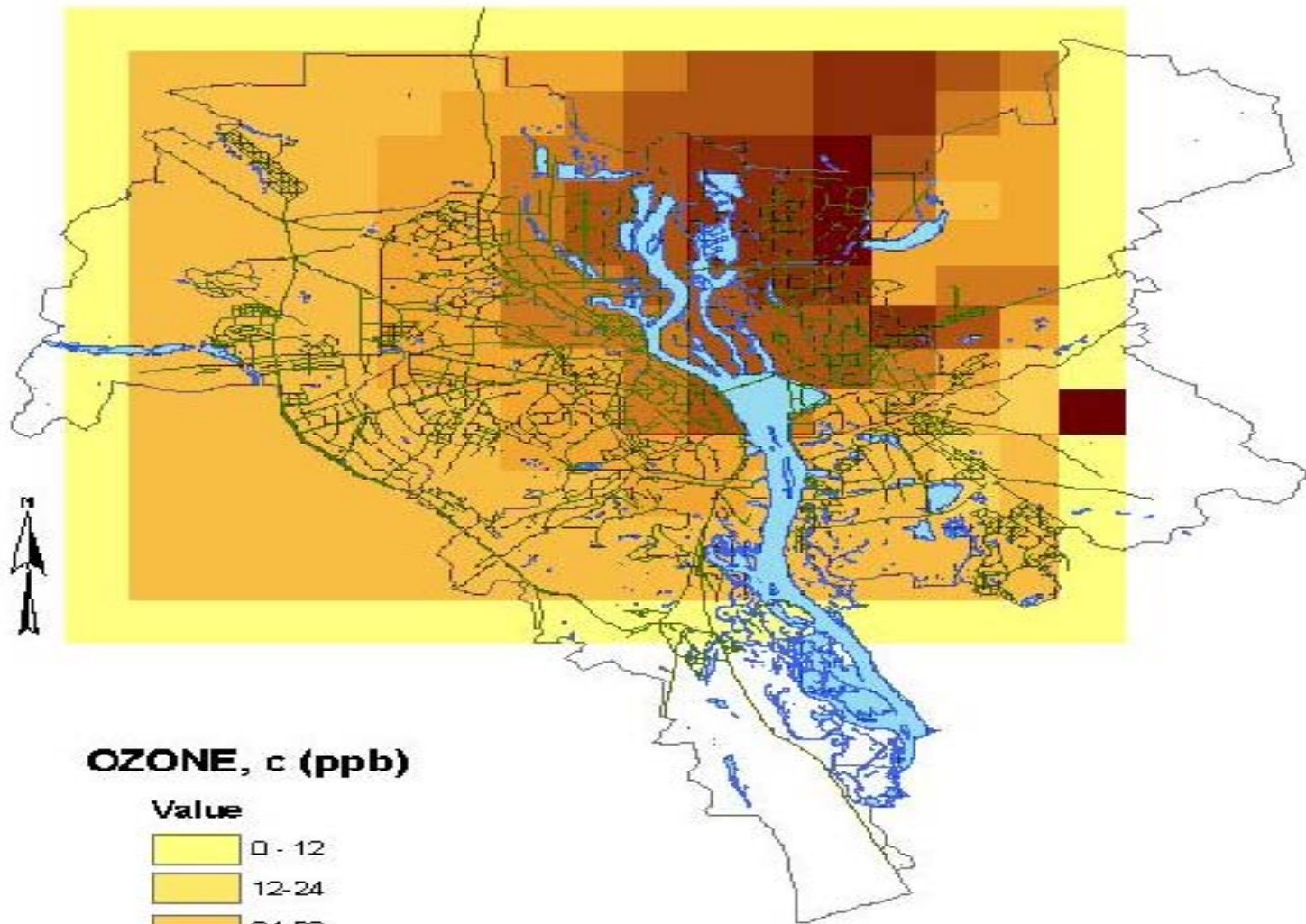
OZONE, c (ppb)

Value

	0 - 12
	12-24
	24-36
	36-48
	48-60
	60-72
	72-84
	84-96
	96-108

0   10 850 Meters
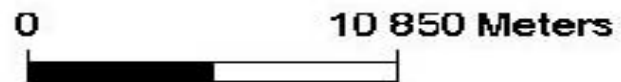
OZONE modelling results and Human Health risks ASSESSMENT

The modeled ozone distribution (for 19 Aug 2000, 14 h) demonstrates that the area of the National Botanic Garden is possibly not the most polluted (1-hour average ozone concentration about 60 ppb). Other parts of Kiev (north-east) can be characterized (Figure 4) by more enhanced ozone concentrations (predicted up to 104 ppb), which exceed European threshold (1hour average) for population information (90 ppb). Note, that 98.7 ppb was observed in National Botanic Garden in August 2007.

It is important task to evaluate possible damage for ecosystems and for population. For human population, a wide variety of physiological responses to ozone have to be considered. The responses are both individually differing, and similar in some population groups. Groups with similarities in their reactions are important to identify, as they may represent those individuals more sensitive to elevated exposures. Population groups that are often mentioned as more sensitive include younger children, child and adult asthmatics, exercising individuals, or individuals exposed to higher temperature and/or humidity. The layers of map of Kiev city and its nearest surroundings in GIS can be used for estimating of exposures of the city population to ozone.
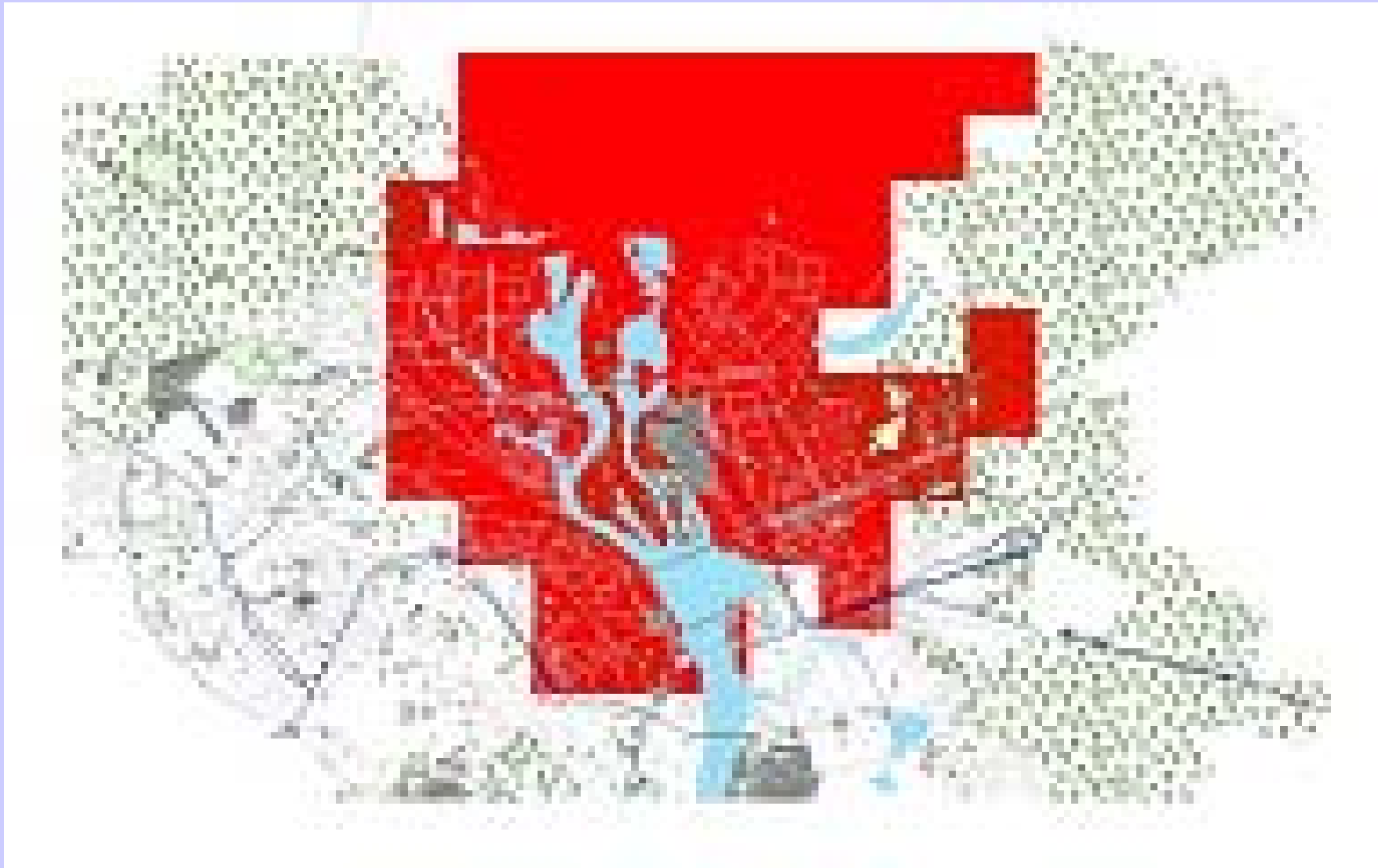
Figure 5. The map of calculated ozone concentration exceeded 60 ppb (red area) for ozone episode in Kiev on 19 August 2000 during 8 hours.

The map of Kiev area with calculated ozone concentrations exceeding 60 ppb (European threshold value[8]) during 8-hour (10.00–18.00) is shown in the figure 5. To estimate possibility of damage for various population groups the risk analysis approach was applied.

The ecological risk assessment may be expressed by the formula[9]:

$$R = Y \times p \qquad (1)$$

Y- risk level: damage value (which is proportional to exceedance of averaged for 8h exposure over threshold),

p - risk factor as probability of damage per a time period.

It is necessary to define particular risk estimate from ozone for different population groups and ecosystems. It can be done by the way of the epidemiological and toxicological researches, that together with ozone exposure modeling and measurement give us the information about danger of exposures and ways of risks reducing. The value of damage is determined by the concentration and toxicity of pollutant:

$$Y = (\sum_{1}^{N} M_i \times K_i) \times K_L \qquad (2)$$

N- number of exceedances of threshold value,

M_i – concentration of pollutant for i-case of exceedance, K_i- coefficient of relative ecological and economical danger of air pollution,

K_L- local coefficient of ecological situation and ecological consequences for the area.

- Value of Ki linked to such parameters as population density, residential and recreation areas and concentrations of others pollutants; KL depend of exposure time. Risks levels for Kiev population, estimated for the ozone episode of August 2000, are presented in the figure 6. Risk level in each cell was calculated relating to population exposure. Higher risk levels are observed in the central part of the city.

- There are two ways to reduce risk level: the first is to restrict exposure (for example by information of the population) and another one is to reduce ozone concentration using anthropogenic emission optimization.

Figure 6. The local risk levels of surface ozone exposure estimated for the population of the city during modeling episode. Higher risk levels are correspondent to darker cell color.

Risk level in each cell was calculated relating to population exposure. Higher risk levels are observed in the central part of the city.
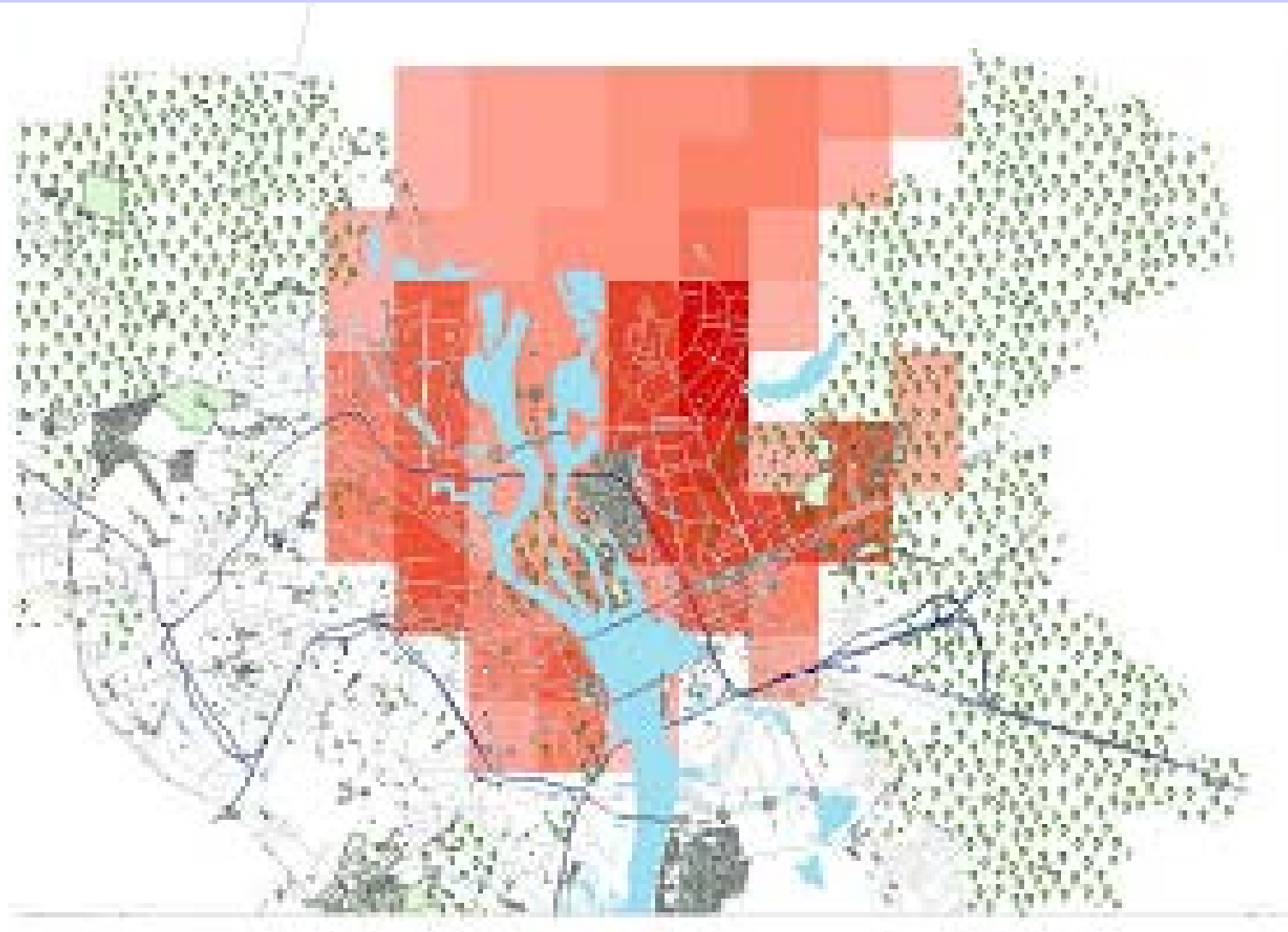
КАРТА МАКСИМАЛЬНОЇ ЗАБРУДНЕНОСТІ м. КИЄВА ПРИЗЕМНИМ ОЗОНОМ (20.08.2000)

	1	2	3	4	5	6	7	8	9	10	11	12	13	14	15	16	17
a	0	0	0	0	0	0	0	0	0	0	0	0	0	0	0	0	0
b	0	39,1	39,4	40,9	42,1	45,2	48,2	52,4	60,2	72,2	75,3	83,0	86,6	91,8	82,5	67,6	0
c	0	39,2	39,1	41,7	43,5	48,1	50,1	57,6	67,6	79,1	75,5	84,0	93,5	93,4	73,8	57,7	0
d	0	39,1	39,3	42,9	44,5	64,8	52,7	60,7	71,1	78,7	85,1	85,0	101,8	87,9	70,8	57,5	0
e	0	38,4	40,0	43,7	45,8	51,9	55,6	55,2	75,9	83,3	84,8	89,0	104,6	86,3	70,0	58,9	0
f	0	38,3	40,1	44,0	47,0	53,0	57,3	65,8	77,2	84,2	84,9	87,4	100,7	79,4	68,9	62,3	0
g	0	38,7	42,2	43,8	46,2	50,6	55,9	65,9	72,1	73,3	88,8	87,5	92,2	76,9	78,1	65,4	0
h	0	40,0	42,0	42,6	46,9	50,9	55,6	64,0	67,1	71,1	79,7	81,2	82,5	85,0	80,0	58,0	0
i	0	40,2	41,1	42,1	47,1	48,6	51,1	58,0	60,3	64,2	81,1	77,1	74,9	60,2	63,5	41,6	0
j	0	38,6	38,4	39,6	43,0	42,5	44,9	53,2	56,9	62,9	73,7	61,4	60,3	53,7	58,2	32,2	0
k	0	39,0	40,0	40,3	41,8	41,0	42,9	50,0	52,5	56,7	59,6	56,7	48,3	50,6	39,4	45,3	0
l	0	39,1	39,2	39,3	40,0	39,5	40,7	46,7	47,7	50,3	50,7	43,9	44,3	42,3	39,3	42,1	0
m	0	39,1	39,1	39,2	39,4	38,5	42,2	45,7	40,1	48,3	47,2	42,2	40,8	38,6	42,8	43,1	0
n	0	39,0	39,0	38,9	38,7	38,8	40,0	38,7	38,8	40,9	39,3	39,3	39,6	40,5	40,0	39,3	0
o	0	0	0	0	0	0	0	0	0	0	0	0	0	0	0	0	0

Райони м. Києва:

1. Ватутінський
2. Дарницький
3. Дніпровський
4. Жовтневий
5. Залізничний
6. Ленінградський
7. Мінський
8. Московський
9. Печерський
10. Подільський
11. Радянський
12. Старокиївський
13. Харківський
14. Шевченківський

ВІДНОСНІ РИЗИКИ ЗАХВОРЮВАНОСТІ НА ПАТОЛОГІЇ СЗД

			Райони м. Києва, 2000 р.												
			Центральні райони						«Спальні» райони						
			Жовт невий	Залі зни чний	Пече рськ ий	Радя нськ ий	Ст аро київ ськ ий	Ш ев че нкі вс ьк ий	Ват утін ськи й	Дар ниц ьки й	Дніп ров ськи й	Лені нгра дськ ий	Мінс ький	Моск овсь кий	По ді ль сь ки й	Хар ківс ьки й
П о к а з н и к и с т а н у С З Д	Д о р о с л і	хвороб и органів диханн я	0,8	1,1	0,95	0,9	0,7	1	2,1	1,9	2,1	1,3	1,26	1,6	1	1,2
		Пневмо-нія	0,7	1,3	1,3	0,9	1,9	1	2,5	2,3	2,5	1,3	2,3	1,7	1	1,6
	Д і т и	Астма-тичний бронхіт	1,2	2,2	1,5	1,1	1,9	1	1,5	2,1	1,4	0,8	1,2	0,76	1	1,1

Найважливішим результатом роботи можна вважати те, що при всіх варіантах дослідження спостерігається наявність статистично достовірних позитивних зв'язків між розрахованими загальними порайонними експозиціями до озону та показниками системи дихання мешканців районів Києва «хвороби органів дихання» та «пневмоніяї» у дорослих, працездатних, пенсіонерів; «астматичний бронхіт» - у дітей. Визначення відносних порайонних ризиків захворюваності на зазначені вище патології системи дихання дали можливість виявити райони міста найбільш небезпечні у цьому сенсі

Results

Two days simulation of ozone episode for 19-20 August 2000 were performed scaling emission data averaged daily and hourly on the basis of annual volumes. Preliminary results of analysis of the first steps of modelling permit to do some main conclusions relative to formation of surface ozone in Kiev city. The comparison of calculated with UAM-V ozone concentrations (ppb) and data of measurements in Botanic Garden shows non-linear variations of O3 concentrations depending on average hourly NOx emission data.

A rather high ozone concentrations exceeding Ukrainian and European limit values were predicted for north-east part of city.

The results of model calculations show an importance of more detailed temporal modulation of emission data, in particular hourly NO, NO2 and VOC data, and the necessity of taking into account night time heterogeneous chemistry.

CONCLUSIONS

As a rule, minimum ozone values are observed in the morning, about 8 hour, maximum - at noonday, 13-15 hours. It was revealed that situations of nocturnal decrease of O to minimum value (about zero) were almost not observed. Contrary, at night it is often observed the second maximum of surface ozone. One of possible explanations of this phenomenon -sinking of ozone from boundary level and specific location of monitoring station - Botanic Garden.

The first results of ozone concentration modelling justify the existence of **two type of ozone forming areas for Kiev city, NO and VOC sensitive**. For Botanic Garden measured ozone concentration at 19-20 August 2000 we reveal non-linear sensitivity to NOx both increase and reduction of NO emission data result in decreasing of O_3 maximum values. Maximal ozone concentrations can be observed in the **residential suburbs**.

Two-step night lowering could be simulated by additional night rejection of NO, for example, by industrial stack in weekend or biomass firing, which can be expected in second half of August. **The night time heterogeneous reactions** must be also considered, especially the processes of ozone uptake and oxidation on the surfaces of condensing water drops or particles of soot. The relevant module of heterogeneous chemistry should be implemented in UAM-V model.

1. Микульская И.А., А.В.Шаврина,Сосонкин М.Г., Волков Ю.Н. -

К оценке влияния степени загрязнения городского воздуха на здоровье горожан

(Наукові праці 2-ої конференції з міжнародною участю «Информаційні тех.-нології в охороні здо-ров'я та практичної медицини",Київ, 2002, с.109-111

- **(Mikulskaya I.A., Shavrina A., Sosonkin M., Volkov Yu.N. On the estimation of the influence of urban air pollution levels on the health of the peoples. Proc. 2 Int. Conf. " Informayional Technologies in the human health protection and applied medicine ", Kiev, 2002, pp. 109-111.)**

2. Sosonkin M., Blum O., Dyachuk V., Shavrina A., Veles A.   Ground-level ozone formation in the Kiev city - in Symp. Eurotrac-2, 2002,   Garmish-Partenkirchen, Germany (abstract, SAT-32 and CD - full text)

3. A.S.Gasanov, M.G.Sosonkin, A.V.Shavrina, V.A.Dyachuk Surface ozone in   the Kiev city, factors and conditions of its formation, sources and sinks. -   Proceedings of the Sixth Baku International Congress, "Energy, Ecology, Economy", Baku 2002

 4.Я.С.Яцкив, А.А.Жалило, В.Р.Суберляк, М.Г.Сосонкин, В.Д.Дячук, А.В.Шаврина, Н.В.Саданова, С.Н.Флерко, А.М.Лукьянов, А.Е.Вольвач, Ю.Л.Кокурин, Л.С.Штирберг Региональная система геодинамического мониторинга Крыма с использованием GNSS Медисциплинарная проблемно-ориентированная программа . **Іновaційні технолоuіi, 2003, Т1.N4-5.С.21-88**.

5. О.Б. Блюм, И.В. Дудак, В.А. Дячук, М.Г. Сосонкін, А.В.Шаврина: Приземний озон у Киеві, умови його накопичення і стоку.-Праці УКР НДГМИ, **Вып.249, 2003**

6. Шаврина   А., Велес А., Сосонкин М., Дячук Измерение и моделирование озона и парниковых газовКФНТ. Приложение**. 2003, №4, 248-2530,2**

7. Шаврина А**.,**Велес А., Сосонкин М., Дячук В Тропоферный озон как опасный загрязнитель атмосфер. КФНТ. Приложение. **2003, №4, 254-2580**

6. M.G. Sosonkin, A.V.Shavrina, A.A. Veles, V.A. Dyachuk, O.B.Blum,   V.I.Nochaj. The study of surface ozone for Kiev city. Proceedings of the   4th International Conference on Urban Air Quality: Measurement, Modelling and   Management. Ranjeet S. Sokhi and Josef Brechler (Editors). Charles University,

   Prague, 25-27 March 2003, pp. 106-109

7. A.V.Shavrina, Sosonkin M.G, Veles A.A.Dyachuk V.ABlum O.B.Nochvaj.The study of surface ozone for Kiev city-Proc.4th Intern. Conf.Urban Air Quality,Prague, 2003. P.106-1090,15.

8. Shavrina A.V., Veles A., Dyachuk V.A., Nochvaj V. NATO Advanced Study Snstitute (NATO ASI. 980064). "Flow and transport processes in complex obstructed geometries: from cities and vegetative canopies to industrial problems. Ukraine, Kyiv, May 4-15, 2004. Paper: Surface ozone modeling with wind field and orography in Kyiv.

9. Ночвай В.І., Шавріна А.В., Дячук В.А., Сосонкін М.Г. Використання ГІС   для моделювання концентрацій приземного озону   CDI праці міжнародної конференції користувачів програмних продуктів ESRI и

   Leica Geosystems в Україні. Ялта- 2004   Веб-сайт: http://www.ecomm.kiev.ua/gis/yalta2003/materials.htm
(Участь і доповідь в міжнародній конференції користувачів програмних продуктів ESRI и Leica Geosystems в Україні „Ялта 2004" присвячений сучасним інформаційним процесам в науках про землю. Доповідь «Оцінка приземного озону в атмосферному повітрі в м. Києві» визнана кращою у секції).

10. В.І. Ночвай, М.Г. Сосонкін, А.В. Шавріна. Використання ГІС для моделювання концентрацій приземого озону // Учені записки ТНУ. Серія: Географічна, 2003.-Ч.16(55).№2.-С.110-114.

11. В.І. Ночвай, М.Г. Сосонкін, А.В. Шавріна. Використання ГІС для підготовки і аналізу просторових даних в моделі розрахунку концентрації приземного озону // Теоретичні та прикладні аспекти геоінформатики. Збірник наукових праць – Київ, 2004. –Т. 2. – С.45-4910.

13. Шавріна А.В., Сосонкін М.Г., Ночвай В.І., Велес О.О. Комплексне геоінформаційне моделювання ризиків шкідливого впливу приземного озону на екосистему міста // Моделювання та інформаційні технології: Збірник наукових праць. – Інститут проблем моделювання в енергетиці, Київ, 2006 – вип.38. – С.109-115

14. Микульская И.А., Шаврина А.В., Кифоренко С.И., Пустовойт О.Г., Волков Ю.Н. Технология оценивания опасного действия приземного озона на здоровье граждан современных мегаполисов. Форум з міжнародною участю "Інформаційні технології в охороні здоров"я та практичній медицині".31 березня 2006 р., м. Київ-2006.

15. Котова А.Б., Белов В.М. Микульская И.А., Пустовойт О.Г. Информационные технологии в процессе тестирования системы внешнего дыхания.1У Міжнародна конференція, молодіжний форум "Єдиний інформаційний простір - 2006" Грудень 2006 р. Дніпропетровськ

16. Котова А.Б., Белов В.М., Кифоренко С.И. Основи стратегии здоровья. Інформаційні технології і кібернетика. Збірник матеріалів 4-ї науково-практичної конференції, Дніпропетровськ, 2006.

**17. A.V. SHAVRINA , M.G. SOSONKIN, A.A. VELES, V.I. NOCHVAY
INTEGRATED MODELLING OF SURFACE AND TROPOSPHERIC OZONE FOR KIEV CITY (accepted to PUBL. NATO CONF., 2007)** (publication date – October 2008)

18. Микульска І.О., Шавріна А.В., Кіфоренко С.І. **Забрудненість міста Києва приземним озоном як медико-єкологічна проблема. – Сб. "Біомедичні Ірформаційні технології в охороне**
здоров'я. БМІТ-2008.

An investigation of ozone and planetary boundary layer dynamics over the complex topography of Grenoble combining measurements and modeling

O. Couach[1], I. Balin[1], R. Jiménez[1], P. Ristori[1], S. Perego[2], F. Kirchner[1], V. Simeonov[1], B. Calpini[3], and H. van den Bergh[1]
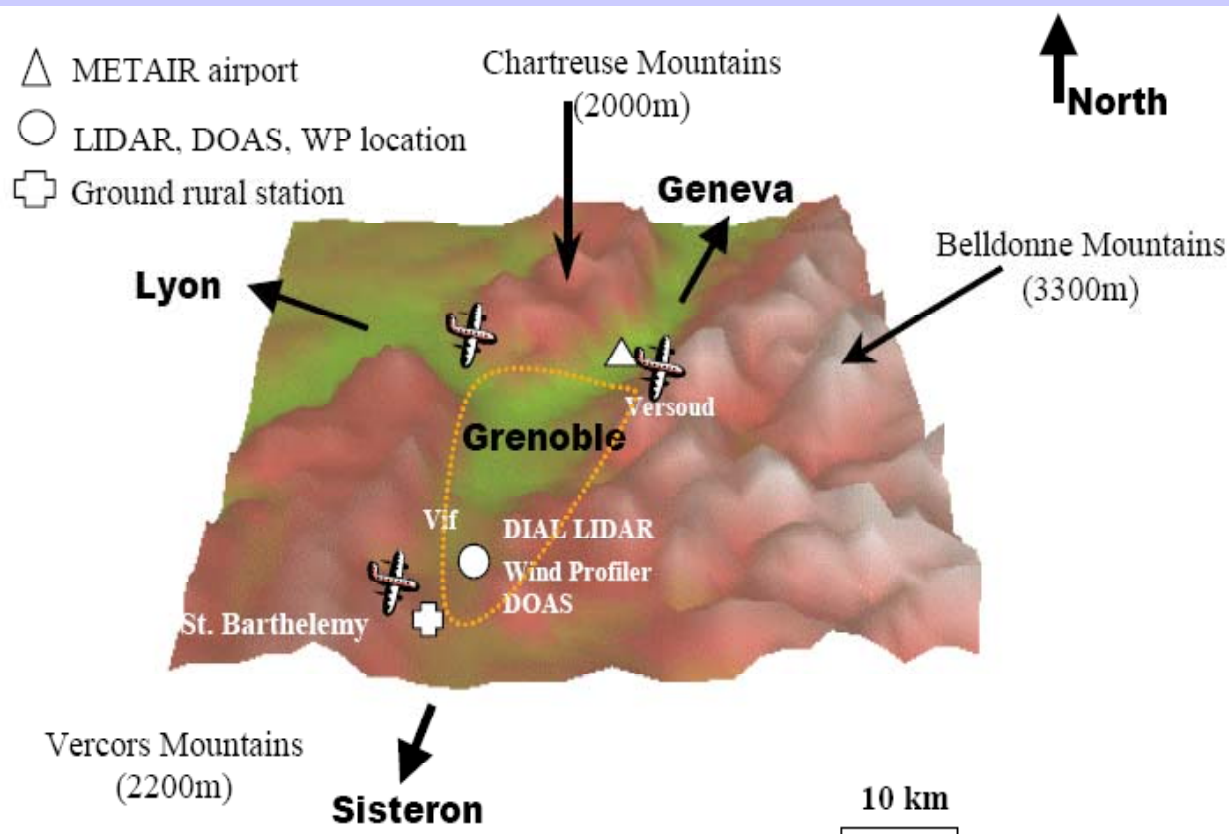
Fig. 1. Topography and locations of fixed instruments and flight path in the Grenoble modeling domain: the Belledone Mountains to the East, the Charteuse massif to the North and the Vercors to the West. Horizontal extent is 68×78 km and the horizontal grid cell size for this domain was 2 km.

Ozone was measured at two stations at 30 km and respectively 20 km South of Grenoble city: St-Barthélémy at 620 m ASL and Vif at 310 m ASL (see Fig. 1). At St-Barthélémy the ozone was measured using a Dasibi ozone point monitor (+/− 1 ppb precision), which is based on ozone UV absorption at 254 nm. Ozone measurements at Vif were performed with the Differential Optical Absorption Spectroscopy (DOAS 2000 Thermo Environmental Instr.) system. The DOAS system uses the ozone UV differential absorption (267–299 nm) along a 1000 m integrated optical path with +/− 1 ppb precision (Jiménez et al., 2001).

(d) Lidar Dial Ozone
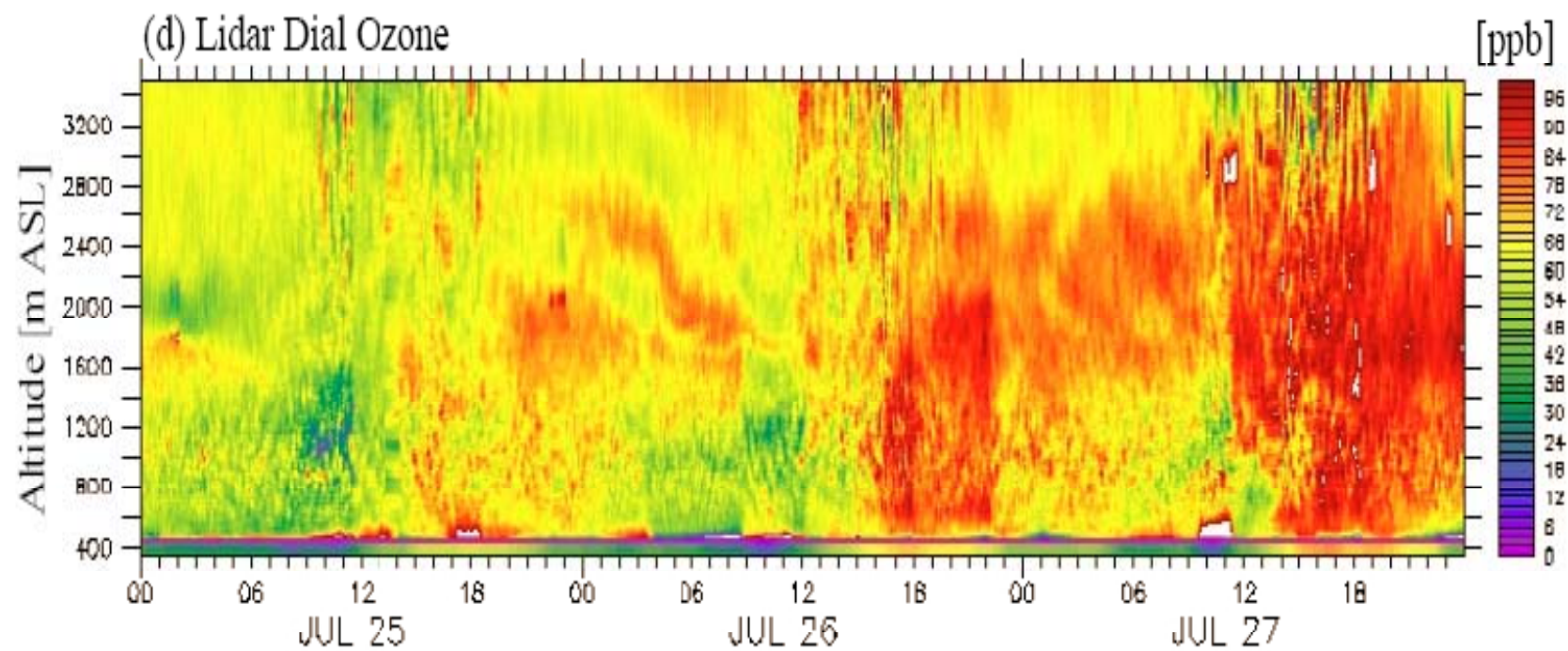
The residual layer as well as the daily variation of the ozone concentration above Vif is presented

3   Modeling approach

The air quality model METeorological PHOtochemistry MODel (METPHOMOD) is used here to investigate the spatial and temporal patterns of air pollution during GRENOPHOT 1999. This model has both a meteorological module, which calculates wind, potential temperature and humidity fields, as well as an atmospheric chemistry module to compute transport and chemical reactions (Perego, 1999). The chemical module is based on the Regional Atmospheric Chemical Mechanism (RACM), a lumped species mechanism (Stockwell et al., 1997).

An investigation of ozone and planetary boundary layer dynamics over the complex topography of Grenoble combining measurements and modeling

O. Couach[1], I. Balin[1], R. Jiménez[1], P. Ristori[1], S. Perego[2], F. Kirchner[1], V. Simeonov[1], B. Calpini[3], and H. van den Bergh[1]

GRENOPHOT 99 POI1

400 m ASL – Ozone [ppb]
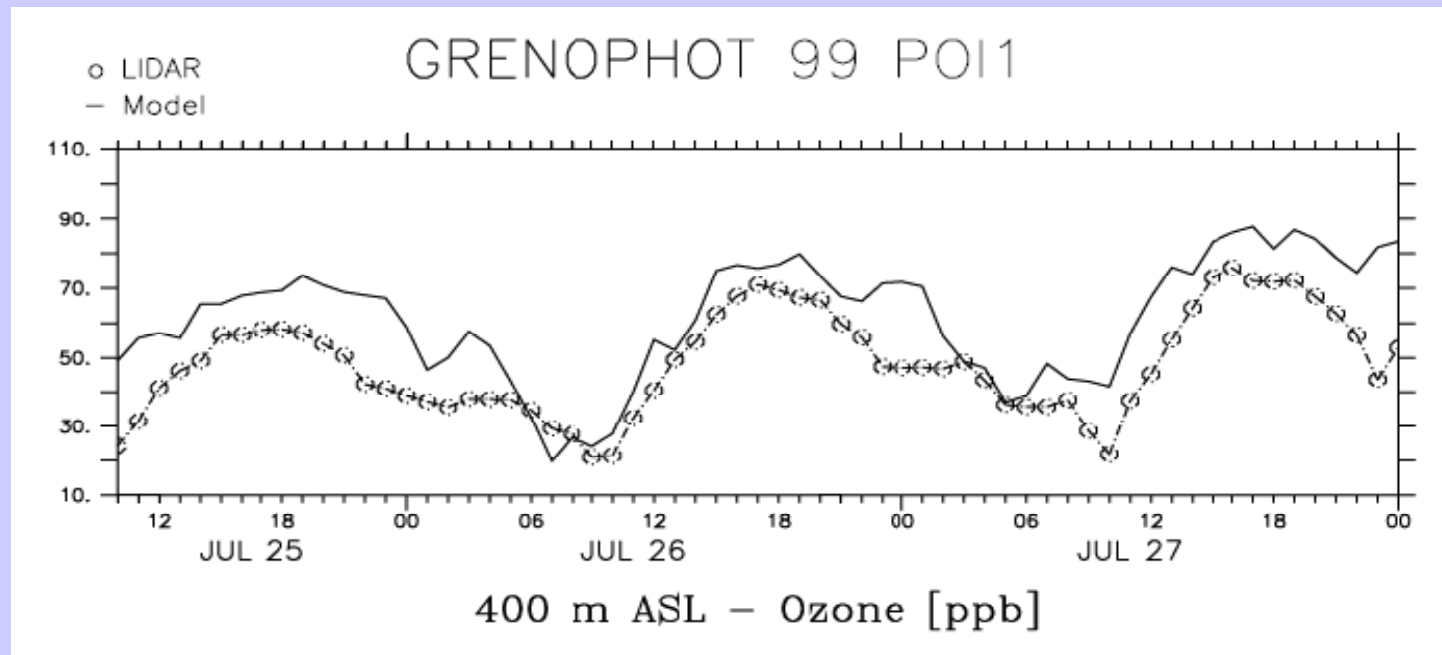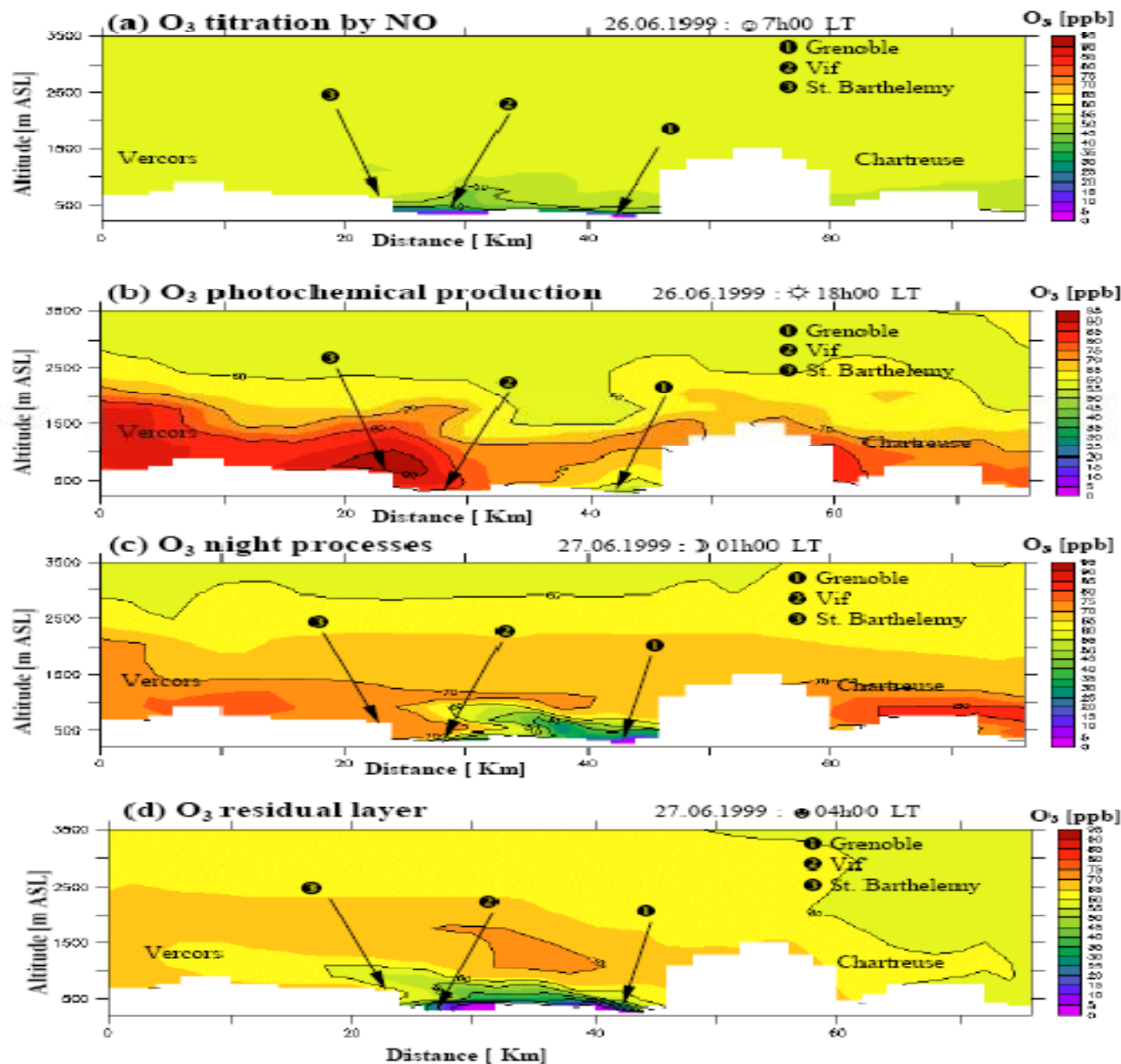
Fig. 10. Simulated ozone dynamics in a south to north (Vif − Grenoble) 50 km transect from the ground to 3500 m ASL on the vertical dimension. The ozone NO titration in the morning (a), the ozone photochemical production (b), the night ozone processes (c) and the ozone residual layer formation (d) are represented here.

THE VARIABLE-GRID

URBAN AIRSHED MODEL (UAM-V)

Prepared by

Systems Applications International, Inc.

a subsidiary of ICF Consulting

California

1. INTRODUCTION

The Urban Airshed Model (UAM) program was originally developed by Systems Applications International (SAI) and has been maintained by SAI for over 25 years. Its roots extend back to the earliest attempts at photochemical air quality modeling in the early 1970s. Since that time, the model has undergone a nearly continuous process of application, comprehensive performance evaluation, update, extension, and improvement.

The variable-grid Urban Airshed Model (UAM-V) system is the most current operational version of the UAM model. It incorporates multiple two-way grid nesting, allowing regional-scale ozone and precursor pollutant transport and several urban areas to be treated within a single modeling domain. In addition, the UAM-V program allows variability in the number and spacing of vertical layers, specification of three-dimensional meteorological variables, and explicit treatment of subgrid-scale photochemical plumes (i.e., plume-in-grid treatment). The UAM software was completely rewritten in a modular form for the UAM-V version, and includes updated deposition, plume-rise, solar flux, and chemical kinetics modules.

SAI has also developed input preparation packages with technical features commensurate with the requirements of the UAM-V system. These include a prognostic meteorological model with four-dimensional data assimilation (Douglas et al., 1991; Myers et al., 1991a) and a complete gridded emission inventory preparation system (Morris, Myers, and Haney, 1990; SAI, 1992). The UAM-V Postprocessing System (UPS) has also been developed to examine model output and assess model performance (SAI, 1996).

Conceptual Overview of the Model

The UAM-V model is a three-dimensional photochemical grid model designed to calculate the concentrations of both inert and chemically reactive pollutants by simulating the physical and chemical processes in the atmosphere that affect pollutant concentrations. The basis for the model is the atmospheric diffusion or species continuity equation. This equation represents a mass balance in which all of the relevant emissions, transport, diffusion, chemical reactions, and removal processes are expressed in mathematical terms. The model is usually exercised over a 48- to 120-hour ozone episode period.

The major factors that affect ozone air quality include:

- The spatial and temporal distribution of emissions of NO_x and volatile organic compounds (VOC) (both anthropogenic and biogenic).

- The composition of the emitted VOC and NO_x.

- The spatial and temporal variations in the wind fields.

- The dynamics of the boundary layer, including stability and the level of mixing.

- The chemical reactions involving VOC, NO_x, and other important species.

- The diurnal variations of solar insolation and temperature.

- The loss of ozone and ozone precursors by dry and wet deposition.

- The ambient background of VOC, NO_x, and other species in, immediately upwind, and above the region of study.

The UAM-V model simulates these processes when it is used to calculate ozone concentrations. It can also be used to simulate carbon monoxide concentrations in an urban area, a simulation that involves no chemical reactions. The model solves the species continuity equation using the method of fractional steps, in which the individual terms in the equation are solved separately in the following order: emissions are injected; horizontal advection/diffusion is solved; vertical advection/diffusion and deposition is solved; and chemical transformations are performed for reactive pollutants. The UAM-V program performs this four-step solution procedure during each advective (driving) time step. The maximum advective time step is a function of the grid size and the maximum wind velocity or horizontal diffusion coefficient. Chemistry and vertical diffusion are solved on fractions of the advective time step to keep their individual numerical schemes stable. A typical driving time step for coarse (10-20 km) grid spacing is 10-15 minutes, whereas time steps for fine grid spacing (1-2 km) are on the order of a few minutes.

Because the UAM-V model accounts for spatial and temporal variations as well as differences in the reactivity (speciation) of emissions, it is ideally suited for evaluating the effects of emission control scenarios on urban air quality. The evaluation starts by replicating a historical ozone episode to establish a base-case simulation. Model inputs are prepared from observed meteorological, emission, and air quality data for a particular day or days using prognostic meteorological modeling and/or diagnostic and interpolative modeling techniques. The model is then applied with these inputs and the results are evaluated to determine its performance. Once the model results have been evaluated and determined to perform within prescribed levels, the same meteorological inputs and a *projected* emission inventory can be used to simulate possible future emission scenarios.

1. **Structured modular computer code:** The code is written in modular form for ease of inclusion of new modules and to take advantage of modern computers.

2. **Vertical grid structure:** The vertical layer structure can be arbitrarily defined by the user and is no longer defined from the diffusion break (mixing height). This allows for higher-resolution vertical layers near the surface and better matching with output from prognostic meteorological models, which usually use a terrain-following coordinate system.

3. **Three-dimensional inputs:** Several meteorological variables that were considered spatially constant in the UAM CB-IV (i.e., in the METSCALARS input file) now vary temporally and spatially (e.g., temperature, water vapor, pressure, and photolysis rates). Furthermore, the horizontal diffusivities and vertical turbulent exchange coefficients are now required as input, usually calculated with output from a prognostic meteorological model.

4. **Variable-grid resolution for chemical kinetic calculations:** When conditions permit, the chemistry calculations can be performed on aggregated blocks of cells rather than individual cells to reduce computation time.

5. **Two-way nested grid:** Finer grids can be embedded in coarser grids for more detailed representation of advection/diffusion, chemistry, and emissions. Several levels of nesting can be accommodated.

6. **Update of the CB-IV chemical mechanism:** The Carbon Bond IV chemical mechanism has been updated. The XO_2-HO_2 reaction has been added along with new temperature effects for PAN reactions. In addition, aqueous-phase (cloud) chemistry has been added as an option.

7. **New dry deposition algorithm:** The dry deposition algorithm formulated by Wesely (1989) has been implemented in the UAM-V program. This algorithm is similar to that used by the Regional Acid Deposition Model (RADM).

8. **True Mass Balance:** Concentrations are advected and diffused in the model using units of mass per unit volume rather than volumetric units (parts per million). When a given amount of ppm of a pollutant moves to a grid cell that has a different temperature or

pressure, there is a different amount of mass within the grid cell for the same ppm (ideal gas law). Using mass per unit volume maintains true mass balance in the advection and diffusion.

9. **Plume-in-Grid (PiG):** Emissions from point sources can be treated by a subgrid-scale Lagrangian photochemical plume model. Pollutant mass is released from the subgrid-scale model to the grid model when the plume size is commensurate with a grid cell size.

10. **New Plume Rise Algorithm:** A new plume rise algorithm has been implemented based on the one in the Gaussian dispersion model TUPOS (Turner et al., 1986).

The most recent version of the UAM-V modeling system (version 1.30) maintains the structure of, and backwards compatibility with, the earlier versions of the UAM-V, but includes major additional features. These include:

11. **CB-IV-TOX Chemical Mechanism:** This mechanism is an extension of the CB-IV mechanism, and includes a more detailed treatment of aldehyde chemistry (e.g., acetaldehyde is treated explicitly), the ability to track primary and secondary aldehydes, treatment of selected toxic species, and other improvements.

12. **Standard or Fast Chemistry Solver:** With the selection of a user-input flag, the model will either employ the standard chemistry solver or the fast chemistry solver.

13. **Process Analysis and Integrated Reaction Rates:** With the selection of a user input flag, the model will save detailed information on each of the physical (e.g. deposition, transport, etc.) and chemical transformation processes in each grid cell at each time step, in addition to the final concentration. This diagnostic tool provides for the examination of the contribution of each of the processes on the calculated concentration in a particular cell or group of cells.

Input Data Required by the UAM-V Model

The UAM-V derived pollutant concentrations are calculated from the emissions, advection, and dispersion of precursors and the formation and deposition of pollutants within every grid cell of the modeling domain. To adequately replicate the full three-dimensional structure of the atmosphere during an ozone episode, the UAM-V program requires an hourly and day-specific database for input preparation. Several preprocessing steps to translate raw emissions, meteorological, air quality, and grid-specific data are required to develop final UAM-V input files.

(**Advection -** The transfer of a property of the atmosphere, such as heat, cold, or humidity, by the horizontal movement of an air mass)

Observed air quality data are used to evaluate model predictions. These data may also be used to estimate the initial concentrations and boundary conditions for ozone, NO_x, and volatile organic compounds (VOC). The UAM-V model is usually used to simulate a multiday episode, and the simulation is started during the early morning hours one to three days before the start of episode. Use of start-up days limits the influence of the initial concentrations (which are not well known) on the simulation of the primary episode days.

Cell Aggregation and Grid Nesting

Although cell aggregation and grid nesting are optional, the model requires a definition of the grid structure. If these options are not utilized, an input file must be generated to indicate that only one uniform grid is to be defined, with no chemical cell aggregation.

It may be desirable to reduce computation time by performing chemical calculations on aggregated blocks of cells rather than individual cells. An aggregation input mapping field specifies which cells are to be aggregated. Cell aggregation may be done horizontally or vertically, and may be constant or time-varying.

Data type	UAM-V files
Meteorological	WIND (x, y-components of winds) TEMPERATURE (3D array of temperature) H2O (3D array of water vapor) VDIFFUSION (3D array of vertical turbulent diffusivity coefficients) HEIGHT (3D arrays of layer heights and pressure) RAIN (2D array of rainfall rates, optional) CLOUD (3D arrays of cloud cover and cloud water content, optional)
Surface characteristics	SURFACE (gridded land use) TERRAIN (terrain heights)
Emissions	EMISSIONS (surface emissions) PTSOURCE (elevated source emissions)
Initial and boundary concentrations	AIRQUALITY (initial concentrations) BOUNDARY (lateral boundary concentrations) TOPCONC (concentrations at the top of the region)
Chemical rates	CHEMPARAM (chemical reaction rates) RATES (tables of photolysis reaction rates) ALBEDO/HAZE/OZCOL (gridded albedo, haze and ozone column data)
Control	CONTROL (simulation control information) AGGMAP (cell aggregation) PACONTROL (process analysis control information)

Layer Heights and Pressure

The UAM-V grid contains a fixed number of vertical layers whose thickness can vary in space or time. The heights above ground level of the layer interfaces, and the atmospheric pressure at layer midpoints, at each horizontal grid location must be specified hourly. These values are usually determined to be consistent with the grid structure used in a prognostic meteorological model that is used to provide the meteorological inputs to the UAM-V program.

Land-Use Type and Surface Albedo

The percent coverage of 11 coded land-use categories are specified at each horizontal grid location for use in the dry deposition calculations. Land-use categories are typically obtained by averaging raw data from a geographic information system for each grid cell.

Gridded surface albedo indices based on land-use categories are also required for each horizontal grid location. These indices, which cross-reference the albedo values used in the photolysis rate preprocessor, are used to locate the proper photochemical reaction rates (or J-values) for the internal calculation of photolysis rates.

Table 4-6.
Land-use categories recognized by UAM-V
Surface roughness and UV albedo values are given for each category.

Category Number	Land-Use Category	Surface Roughness (meters)	UV Albedo
1	Urban	3.00	0.08
2	Agricultural	0.25	0.05
3	Range	0.05	0.05
4	Deciduous forest	1.00	0.05
5	Coniferous forest including wetland	1.00	0.05
6	Mixed forest	1.00	0.05
7	Water	0.0001	0.04
8	Barren land	0.002	0.08
9	Nonforest wetlands	0.15	0.05
10	Mixed agricultural and range	0.10	0.05
11	Rocky (low shrubs)	0.10	0.05

Preprocessors are available to develop the surface file from USGS or other land-use data (PRELND or POSTLND, depending on the type of USGS data used). These preprocessors are described elsewhere.

2. TECHNICAL FORMULATION

The variable-grid Urban Airshed Model (UAM-V) system is a three-dimensional grid (Eulerian) model designed to calculate the concentrations of both inert and chemically reactive pollutants by simulating the physical and chemical processes in the atmosphere that affect pollutant concentrations. The basis for the UAM-V model is the atmospheric diffusion equation (also called the species continuity or advection/diffusion equation). This equation represents a mass balance in which all of the relevant emissions, transport, diffusion, chemical reactions, and removal processes are expressed in mathematical terms as follows:

$$\underbrace{\frac{\partial c_i}{\partial t}}_{\substack{\text{Time} \\ \text{Dependence}}} + \underbrace{\frac{\partial(uc_i)}{\partial x} + \frac{\partial(vc_i)}{\partial y} + \frac{\partial(wc_i)}{\partial z}}_{\text{Advection}} = \underbrace{\frac{\partial}{\partial x}\left(K_X\frac{\partial c_i}{\partial x}\right) + \frac{\partial}{\partial y}\left(K_Y\frac{\partial c_i}{\partial y}\right) + \frac{\partial}{\partial z}\left(K_V\frac{\partial c_i}{\partial z}\right)}_{\text{Turbulent Diffusion}}$$

$$+ \underbrace{R_i}_{\substack{\text{Chemical} \\ \text{Reaction}}} + \underbrace{S_i}_{\text{Emissions}} + \underbrace{D_i}_{\substack{\text{Dry} \\ \text{Deposition}}} + \underbrace{W_i}_{\substack{\text{Wet} \\ \text{Deposition}}}$$

where

c_i	=	concentration of pollutant i, a function of space (x,y,z) and time (t)
u,v,w	=	horizontal and vertical wind speed components
K_X, K_Y	=	horizontal turbulent diffusion coefficients
K_V	=	vertical turbulent exchange coefficients
R_i	=	net rate of production of pollutant i by chemical reactions
S_i	=	emission rate of pollutant i
D_i	=	net rate of change of pollutant i due to surface uptake processes
W_i	=	net rate of change of pollutant i due to wet deposition processes

The model employs finite-difference numerical techniques for the solution of the advection/diffusion equation. The region to be simulated is divided into several three-dimensional grids covering the region of interest. A base coarse grid covering the entire domain must first be defined; then finer nested grids within the coarse grid may be defined for regions in which more refined analyses are desired. The model accepts nesting in both the horizontal and vertical, allowing for many levels of nesting if desired.

The vertical layer structure of the UAM-V model can be defined arbitrarily by the user. Usually, the vertical layers are defined to match the vertical layer structure of the meteorological model used to generate the UAM-V meteorological inputs (note that unlike previous versions of the UAM model, the vertical structure is not dependent on the mixing height). The UAM-V grid nesting in the vertical allows for the use of high resolution in regions where it is needed. For example, five vertical layers could be specified to resolve synoptic-scale transport and any other important features (e.g., a nocturnal jet) in the outer coarse grid region and 8–12 vertical layers could be defined in the innermost fine grid where high vertical resolution is needed to resolve complex transport features due to topographic or ocean/lake breeze effects.

Atmospheric Chemistry

Gas-Phase Chemistry

Ozone is formed in the atmosphere through chemical reactions between nitrogen oxides (NO_x) and volatile organic compounds (VOC). Hundreds of organic compounds and thousands of reactions participate in the formation of ozone in the atmosphere. The explicit treatment of all of these compounds and reactions would be prohibitively complex in a Eulerian-based grid model such as the UAM program. Thus most photochemical chemical kinetic mechanisms treat organic compounds in groups, often on the basis of the reactive functional groups they contain.

The UAM-V program employs an extension of version IV of the Carbon Bond Mechanism (CB-IV) for solving chemical kinetics (Gery et al., 1988). This extension called CB-IV-TOX expands the treatment of olefins and aldehydes including an explicit treatment of acetaldehyde. The carbon-bond approach disaggregates organic species based on the carbon bonds of the organic compounds. For example, propylene, butene, and 1-pentene each have one terminal olefinic carbon double bond but the number of single carbon bonds are different. Thus, in the carbon-bond approach propylene, butene, and 1-pentene would each be represented by one olefinic bond (OLE) and one, two, and three paraffinic bonds (PAR), respectively.

As implemented here, the CB-IV-TOX contains over 100 reactions and over 30 chemical species. The reactions are given in Table 2-1. Table 2-2 lists the species treated by the

Table 2-1.
The Carbon Bond Mechanism, Version IV-TOX, used in the UAM-V model, version 1.30

	Reaction		Rate Constant[a] @ 298 K (ppm^{-n} min^{-1})	E/R (K)
1	NO2	$\rightarrow$ NO + O	Radiation Dependent[b]	
2	O	$\rightarrow$ O3	4,323,000	-1175
3	O3 + NO	$\rightarrow$ NO2	26.64	1370
4	O + NO2	$\rightarrow$ NO	13,750	0
5	O + NO2	$\rightarrow$ NO3	2309	-687
6	O + NO	$\rightarrow$ NO2	2438	-602
7	NO2 + O3	$\rightarrow$ NO3	0.04731	2450
8	O3	$\rightarrow$ O	$0.053 \times k_1$	
9	O3	$\rightarrow$ O1D	Radiation Dependent[b]	
10	O1D	$\rightarrow$ O	424,600	-390
11	O1D + H2O	$\rightarrow$ 2 OH	3.26	0
12	O3 + OH	$\rightarrow$ HO2	100	940
13	O3 + HO2	$\rightarrow$ OH	3	580
14	NO3	$\rightarrow$ 0.89 NO2 + 0.89 O + 0.11 NO	$33.9 \times k_1$	
15	NO3 + NO	$\rightarrow$ 2 NO2	44,160	-250
16	NO3 + NO2	$\rightarrow$ NO + NO2	0.5901	1230
17	NO3 + NO2	$\rightarrow$ N2O5	1853	-256
18	N2O5 + H2O	$\rightarrow$ 2 HNO3	1.9×10^{-6}	0
19	N2O5	$\rightarrow$ NO3 + NO2	2.776	10,900
20	NO + NO	$\rightarrow$ 2 NO2	0.00015	-530

21	NO + NO2 + H2O	→ 2 HONO	3.0×10^{-8}	-6348
22	NO + OH	→ HONO	9799	-806
23	HONO	→ NO + OH	$0.1975 \times k_1$	
24	HONO + OH	→ NO2	9770	0
25	HONO + HONO	→ NO + NO2	0.00002	0
26	NO2 + OH	→ HNO3	16,820	-713
27	HNO3 + OH	→ NO3	217.9	-1000
28	NO + HO2	→ OH + NO2	12,270	-240
29	NO2 + HO2	→ PNA	2025	-749
30	PNA	→ HO2 + NO2	5.115	10,121
31	PNA + OH	→ NO2	6833	-380
32	HO2 + HO2	> H2O2	4144	-1150
33	HO2 + HO2 + H2O	→ H2O2	0.2181	-5800
34	H2O2	→ 2 OH	$0.255 \times k_{39}$	
35	H2O2 + OH	→ HO2	2520	187
36	CO + OH	→ HO2	322	0
37	FORM + OH	→ HO2 + CO	16,300	110
38	FORM	→ 2 HO2 + CO	Radiation Dependent[b]	
39	FORM	→ CO	Radiation Dependent[b]	
40	FORM + O	→ OH + HO2 + CO	237	1550
41	FORM + NO3	→ HNO3 + HO2 + CO	0.93	0
42	ACET + O	→ C2O3 + OH	636	986
43	ACET + OH	→ C2O3	21,900	-205
44	ACET + NO3	→ C2O3 + HNO3	4.03	1860
45	ACET	→ FORM + 2 HO2 + CO + XO2	Radiation Dependent[b]	

No.	Reaction		Products	A	B
46	C2O3 + NO	→	FORM + NO2 + HO2 + XO2	28,200	180
47	C2O3 + NO2	→	PAN	13,700	-380
48	PAN	→	C2O3 + NO2	0.0254	13,500
49	C2O3 + C2O3	→	2 FORM + 2 XO2 + 2 HO2	24,500	-530
50	C2O3 + HO2	→	0.33 O3	20,900	-1040
51	CH4 + OH	→	FORM + XO2 + HO2	10.34	1710
52	PAR + OH	→	0.87 XO2 + 0.13 XO2N + 0.11 HO2 + 0.06 ACET - 0.11 PAR + 0.76 ROR + 0.05 ALDX	1203	0
53	ROR	→	0.96 XO2 + 0.6 ACET + 0.94 HO2 2.1 PAR + 0.04 XO2N + 0.02 ROR + 0.5 ALDX	137,100	8000
54	ROR	→	HO2	95,445	0
55	ROR + NO2	→	NTR	22,000	0
56	OLE + O	→	0.24 ACET + 0.38 HO2 + 0.28 XO2 + 0.3 CO + 0.2 FORM + 0.02 XO2N + 0.22 PAR + 0.2 OH + 0.39 ALDX	5920	324
57	OLE + OH	→	FORM + 0.38 ACET +0.62 ALDX - PAR + XO2 + HO2	42,000	-504
58	OLE + O3	→	0.19 ACET + 0.31 ALDX + 0.74 FORM + 0.22 XO2 + 0.1 OH + 0.33 CO + 0.44 HO2 - PAR	0.018	2105
59	OLE + NO3	→	0.91 XO2 + FORM + 0.09 XO2N + 0.35 ACET + 0.56 ALDX + NO2 - PAR	11.35	0
60	ETH + O	→	FORM + 1.7 HO2 + CO + 0.7 XO2 + 0.3 OH	1080	792
61	ETH + OH	→	XO2 + 1.56 FORM + 0.22 ALDX + HO2	11,920	-411
62	ETH + O3	→	FORM + 0.42 CO + 0.12 HO2	0.0027	2633
63	TOL + OH	→	0.44 HO2 + 0.08 XO2 + 0.36 CRES + 0.56 TO2	9150	-322
64	TO2 + NO	→	0.9 XO2 + 0.9 HO2 + 0.9 OPEN +NO + 0.1 XO2N	12,000	0
65	TO2	→	CRES + HO2	250	0

No.	Reaction		Products	Rate 1	Rate 2
66	CRES + OH	→	0.4 CRO + 0.6 XO2 + 0.6 HO2 + 0.3 OPEN	61,000	0
67	CRES + NO3	→	CRO + HNO3	32,500	0
68	CRO + NO2	→	NPHN	20,000	0
69	OPEN	→	C2O3 + HO2 + CO	$9.04 \times k_{38}$	
70	OPEN + OH	→	XO2 + 2 CO + 2 HO2 + C2O3 + FORM	44,000	0
71	OPEN + O3	→	0.03 ALDX + 0.62 C2O3 + 0.7 FORM + 0.03 XO2 + 0.69 CO + 0.08 OH + 0.76 HO2 + 0.2 MGLY	0.015	500
72	XYL + OH	→	0.7 HO2 + 0.5 XO2 + 0.2 CRES + 0.8 MGLY + 1.1 PAR + 0.3 TO2	36,200	-116
73	MGLY + OH	→	XO2 + C2O3	26,000	0
74	MGLY	→	C2O3 + HO2 + CO	$0.022 \times k_1$	
75	ISOP + O	→	0.75 ISPD + 0.50 FORM + 0.25 X02 + 0.25 HO2 + 0.25 CXO3 + 0.25 PAR	53,200	0
76	ISOP + OH	→	0.912 ISPD + 0.629 FORM + 0.991 XO2 + 0.912 HO2 + 0.088 X02N	147,600	-407.6
77	ISOP + O3	→	0.65 ISPD + 0.60 FORM + 0.20 X02 + 0.066 HO2 + 0.266 OH + 0.20 CXO3 + 0.15 ALDX + 0.35 PAR + 0.066 CO	0.019	1912
78	ISOP + NO3	→	0.20 ISPD + 1.0 X02 + 0.80 HO2 + 0.20 NO2 + 0.80 ALDX + 2.4 PAR + 0.8 NTR	996	448
79	XO2 + NO	→	NO2	12,000	0
80	XO2 + XO2	→		2000	-1300
81	XO2N + NO	→	NTR	12,000	0
82	ETOH + OH	→	HO2 + 0.95 ACET + 0.78 FORM + 0.05 XO2 + 0.011 ALDX	4840	66.8
83	ETOH + NO3	→	HO2 + ACET + HNO3	1.33	0
84	MEOH + OH	→	FORM + HO2	1375	0
85	MEOH + NO3	→	HO2 + FORM + HNO3	0.33	0

86	XO2 + HO2	→		8,900	-1300
87	XO2N + HO2	→		8,900	-1300
88	XO2N + XO2N	→		2,000	-1300
89	XO2N + XO2	→		4,000	-1300
90	ALDX + O	→	CXO3 + OH - PAR	632.	986.
91	ALDX + OH	→	CXO3 - PAR	24000.	-250.
92	ALDX NO3	→	CXO3 + HNO3 - PAR	4.03	1860.
93	ALDX	→	ACET + 2.0 HO2 + CO + XO2 - PAR	Radiation Dependent[b]	
94	IOLE + O	→	1.14 ACET + 0.76 ALDX + 0.1 HO2 + 0.1 XO2 + 0.1 CO + 0.1 PAR	34000.	0.
95	IOLE + OH	→	1.2 ACET + 0.8 ALDX + HO2 + XO2	94300.	-550.
96	IOLE + O3	→	0.60 ACET + 0.40 ALDX + 0.25 FORM + 0.25 CO + 0.5 O + 0.5 OH + 0.5 HO2	0.31	1100.
97	IOLE + NO3	→	1.09 ACET + 0.73 ALDX + HO2 + NO2	573.	270.
98	CXO3 + NO	→	ACET + NO2 + HO2 + XO2	28200.	180.
99	CXO3 + NO2	→	PANX	13700.	-380.
100	PANX	→	CXO3 + NO2	2.54E-2	13500.
101	CXO3 + C2O3	→	ACET + FORM + 2.0 XO2 + 2.0 HO2	24500.	-530.
102	CXO3 + HO2	→	0.33 O3	20900.	-1040.
103	PANX + OH	→	ACET + NO2	1700.	0.
104	OH + HO2	→		1.626E5	-250.
105	ISPD + OH	→	1.565 PAR + 0.167 FORM + 0.713 XO2 + 0.503 HO2 + 0.334 CO + 0.168 MGLY + 0.253 ACET + 0.21 C2O3 + 0.288 CXO3 + 0.021 ALDX	49.660	0
106	ISPD + O3	→	0.114 C2O3 + 0.15 FORM + 0.85 MGLY + 0.154 HO2 + 0.268 OH + 0.064 XO2 + 0.02 ACET + 0.36 PAR + 0.225 CO	0.0105	0

107	ISPD + NO3	→	0.357 ALDX + 0.282 FORM + 1.282 PAR + 0.925 HO2 + 0.643 CO + 0.075 CXO3 + 0.075 XO2 + 0.075 HNO3 + 0.85 NTR	1.478	0
108	ISPD	→	0.333 CO + 0.067 ACET + 0.90 FORM + 0.832 PAR + 1.033 HO2 + 0.70 XO2 + 0.967 C2O3 + 0.7 CXO3	Radiation dependent[b]	
109	ISOP + NO2	→	0.20 ISPD + 1.0 XO2 + 0.80 HO2 + 0.20 NO + 0.80 ALD2 + 2.4 PAR + 0.8 NTR	0.00022	0
110	MTBE + OH	→	1.37 XO2 + 0.98 HO2 + 0.42 FORM + 0.97 PAR + 0.02 XO2N	4100.	0
111	SO2 + OH	→	SULF + HO2	1110	-160
112	SO2	→	SULF	8.167E-5	0

[a] Pressure dependent values for the concentrations of M and O_2 are included in the rate constants where appropriate: $[M] = 10^6$ ppm, $[O_2] = 2.095 \times 10^5$ ppm.

[b] Representative values for the rates of photolysis reactions 1, 9, 38, 39, 45, 93, and 108 are given in Table 2-3.

[c] In the UAM-V, the concentration of methane is assumed to be spatially invariant and therefore $[CH_4]$ of 1.85 ppm is included in the rate constant for reaction 51.

Photolysis Rates

Photochemical models require information on solar radiation in order to calculate photolysis rates for the photochemical reactions that drive the formation of ozone. The CB-IV chemical mechanism implemented in the UAM-V reads in photochemical reaction rates, or J-values, for seven processes: J_{NO2}, J_{O1D}, J_{HCHOr}, J_{HCHOs}, J_{ACETr}, J_{ALDX}, and $J_{Acrolein}$ (reactions 1, 9, 38, 39, 45, 93, and 108 in Table 2-1). Photolysis rates for several other photochemical reactions are derived from these J-values using scaling factors (see Gery et al., 1988).

The photolysis rate for a given process is expressed by the following integral:

$$J_n = \int_{\lambda_{min}}^{\lambda_{max}} I_n(\lambda) \bullet \sigma_n(\lambda) \bullet \phi_n(\lambda) \, d\lambda$$

where $I(\lambda)$ is the wavelength-resolved actinic flux, $\sigma(\lambda)$ is the wavelength-resolved absorption cross-section for the species undergoing photolysis, and $\phi(\lambda)$ is the wavelength-resolved quantum yield for the photolysis process.

Actinic flux $I(\lambda)$ varies in space and time and must therefore be estimated by the UAM-V program. It is a function of the following variables:

1. The extraterrestrial solar flux—a parameterization of the brightness of the sun at the top of the atmosphere (Fröhlich and Werhli, 1983).

2. Surface UV albedo—the amount of UV radiation reflected from the earth's surface, which is land-use dependent.

3. Turbidity—the optical extinction due to scattering and absorption by aerosols.

4. Total O_3 column density over the modeling domain—in Dobson units, latitudinally and seasonally dependent.

For each time step during UAM-V integration, the relevant photolysis rates are determined as follows:

1. The solar zenith angle for the grid cell is calculated based on the latitude/longitude, time of day, and date.

2. The average altitude of the grid cell is taken as the height of the midpoint of the grid cell above ground.

3. The hourly-average cloud cover in tenths of total coverage, the daily-average ozone column index, daily-average turbidity index, and surface albedo index for the grid cell are taken from gridded inputs of all these variables.

4. Indices for ozone column, albedo, and turbidity are used to locate the appropriate J-value look-up table generated by the photolysis rate preprocessor. Photolysis rates for the grid cell are then calculated by linear interpolation between the nearest values of solar zenith angle and altitude in the look-up table.

5. These photolysis rates are then corrected for cloud cover greater than 70% based on factors used in RADM. (Adjustment factors used are as follows for 70%, 80%, 90%, and 100% cloud cover: 0.72, 0.68, 0.64, 0.59.)

Pollutant Transport

Pollutants are transported primarily by advection, that is, by the mean or bulk motion of the air. Accurate representation of the magnitude and variability of the winds within the space-time simulation domain therefore is of key importance in successful application of the UAM-V model.

Advection in the UAM model is treated by specifying horizontal wind fields (i.e., u and v wind components in each grid cell) for each vertical layer and each nested grid. The vertical velocity in the UAM-V terrain-following coordinate system is then calculated from the conservation of mass equation.

The UAM-V model has relied primarily on prognostic meteorological model output to define wind fields, although the model has also been applied using wind fields generated with objective analysis techniques of upper-air and surface meteorological observations (Morris et al., 1991c). To date, the UAM-V has been applied using meteorological fields generated by MM5, MC2, SAIMM, SUMM, and the RAMS prognostic meteorological models.

Grid Nesting

The UAM-V model can provide two-way interactive nesting of fine grids within coarser grids in both the horizontal and the vertical. The fine grids must be nested completely within the coarse grid domain, the edges of the fine grid must correspond to a coarse grid cell edge, and, currently, the fine grids must be rectangular in shape (or trapezoidal if a latitude/longitude coordinate system is being used). The horizontal spacing of a fine grid may be any integral subdivision of the coarser grid within which it is embedded. There may be many fine grids within a coarse grid, and there can be several levels of nesting (i.e., finer grids embedded within an embedded fine grid); however, fine grids cannot overlap each other. This nested-grid approach has been tested to assure accuracy and mass consistency (Morris et al., 1991a,b, 1992a,b; Myers et al., 1991).

Turbulent Diffusion

Diffusion of pollutants in the UAM-V model is assumed to be proportional to the concentration gradient in space (i.e., "K-theory" or "first-order closure"). The proportionality factor is termed the eddy diffusivity coefficient (K_X, K_Y, and K_V in the advection/diffusion equation).

Horizontal diffusivities are calculated within the UAM-V program based on deformation characteristics of the horizontal wind (Smagorinsky, 1963). Scaling factors are applied to the deformation terms based on the square of grid cell resolution; maximum and minimum allowable horizontal diffusivities are specified by the user.

Vertical turbulent exchange coefficients may be diagnosed from the UAM-V wind and temperature fields, or directly interpolated from K_V fields estimated using a prognostic meteorological model.

Zero-flux conditions are specified on all lateral boundaries for horizontal diffusion, and for the top of the model for vertical diffusion. The lower boundary condition for vertical diffusion is specified as the dry deposition flux from layer 1 to the surface.

Surface Removal Processes

The UAM-V dry deposition algorithm is based on the scheme in the RADM model described by Wesely (1989). It is described briefly in the following paragraphs; for more complete descriptions, see Gray et al. (1991) and Scire (1991).

In the model the flux of pollutant material to the lower boundary (surface) (F_0) is expressed as concentration in the first model layer (C_i) times deposition velocity (V_d):

$$F_0 = -C_i V_d$$

The deposition velocity is estimated as an inverse sum of a series of resistances. For gaseous species this is expressed as follows:

$$V_d = \frac{1}{R_a + R_b + R_s}$$

where

R_a = aerodynamic resistance

R_b = boundary layer resistance

R_s = surface resistance

The deposition velocity of particulate species also depends on the size distribution and density of the particles in question. Large particles have a significant sedimentation velocity (V_{sed}) that acts in parallel to the other resistances. Very small particles behave in a manner similar to gases, albeit they diffuse more slowly. The simplistic expression for the particle deposition velocity is as follows:

$$V_d = V_{sed} + \frac{1}{R_a + R_b + R_a R_b V_{sed}}$$

Solar Zenith Angle	Photolysis Rate (min^{-1})						
	J_{NO2}	J_{O1D}	J_{HCHOr}	J_{HCHOs}	J_{ACETr}	$J_{Acrolein}$†	J_{ALDX}
0	5.699×10^{-1}	2.595×10^{-3}	2.129×10^{-3}	2.848×10^{-3}	3.909×10^{-4}	1.117×10^{-4}	1.346×10^{-3}
10	5.654×10^{-1}	2.507×10^{-3}	2.097×10^{-3}	2.816×10^{-3}	3.820×10^{-4}	1.106×10^{-4}	1.319×10^{-3}
20	5.516×10^{-1}	2.252×10^{-3}	1.999×10^{-3}	2.721×10^{-3}	3.558×10^{-4}	1.072×10^{-4}	1.239×10^{-3}
30	5.276×10^{-1}	1.860×10^{-3}	1.834×10^{-3}	2.556×10^{-3}	3.136×10^{-4}	1.014×10^{-4}	1.109×10^{-3}
40	4.913×10^{-1}	1.380×10^{-3}	1.601×10^{-3}	2.314×10^{-3}	2.575×10^{-4}	9.276×10^{-5}	9.324×10^{-4}
50	4.393×10^{-1}	8.798×10^{-4}	1.299×10^{-3}	1.981×10^{-3}	1.912×10^{-4}	8.070×10^{-5}	7.184×10^{-4}
60	3.654×10^{-1}	4.418×10^{-4}	9.335×10^{-4}	1.540×10^{-3}	1.211×10^{-4}	6.432×10^{-5}	4.813×10^{-4}
70	2.597×10^{-1}	1.477×10^{-4}	5.278×10^{-4}	9.798×10^{-4}	5.711×10^{-5}	4.262×10^{-5}	2.480×10^{-4}
78	1.476×10^{-1}	3.856×10^{-5}	2.248×10^{-4}	4.806×10^{-4}	2.010×10^{-5}	2.209×10^{-5}	9.675×10^{-5}
86	4.393×10^{-2}	4.694×10^{-6}	3.916×10^{-5}	1.062×10^{-4}	2.806×10^{-6}	5.541×10^{-6}	1.546×10^{-5}

* Values are calculated for an altitude of 640 m above mean sea level, an ozone column of 300 Dobson units, a surface albedo of 0.05, and an optical depth due to absorption and scattering by atmospheric aerosols of 0.2.

† Used in estimating ISPD photolysis rate.

Meteorological Inputs

Wind Fields (WIND)

The WIND file contains the horizontal wind components (u and v) for each grid cell for each hour of the simulation; these winds determine the transport of simulated pollutants. Additionally, the file defines the surface wind speed at each horizontal grid location (for use in deposition calculations). The vertical (w) wind component is not an input; instead it is calculated directly by the UAM-V from the horizontal wind inputs. Wind fields are usually derived from the output of a meteorological model.

U and V are the horizontal wind components in the x- and y-directions respectively in meters per second. WSURF is the surface wind speed in meters per second.

Temperatures (TEMPERATUR)

The TEMPERATUR file defines the absolute temperature (K) for each grid cell for each hour of the simulation. The absolute temperature governs certain chemical reaction rates in the CB-IV chemical mechanism. This file contains the surface temperature and the temperature at the midpoint of each cell in the coarse grid. The temperature may vary spatially and temporally and is usually based on meteorological model output.

Water Vapor (H2O)

The H2O file contains the concentration of water vapor in parts per million by volume (ppmv) at the midpoint of each cell in the coarse grid. Water vapor concentration may vary spatially and temporally and are usually computed from hourly specific humidity outputs from the meteorological model, vertically averaged within UAM layers, horizontally averaged or interpolated as necessary, and converted to ppmv.

Vertical Turbulent Exchange Coefficients (K_v) (VDIFFUSION)

The VDIFFUSION file defines the vertical turbulent exchange coefficients (or diffusivities) in meters squared per second (applicable to all species) at the top of each cell in the grid system for each hour of the simulation. Vertical exchange coefficients may vary spatially and temporally.

An investigation of ozone and planetary boundary layer dynamics over the complex topography of Grenoble combining measurements and modeling
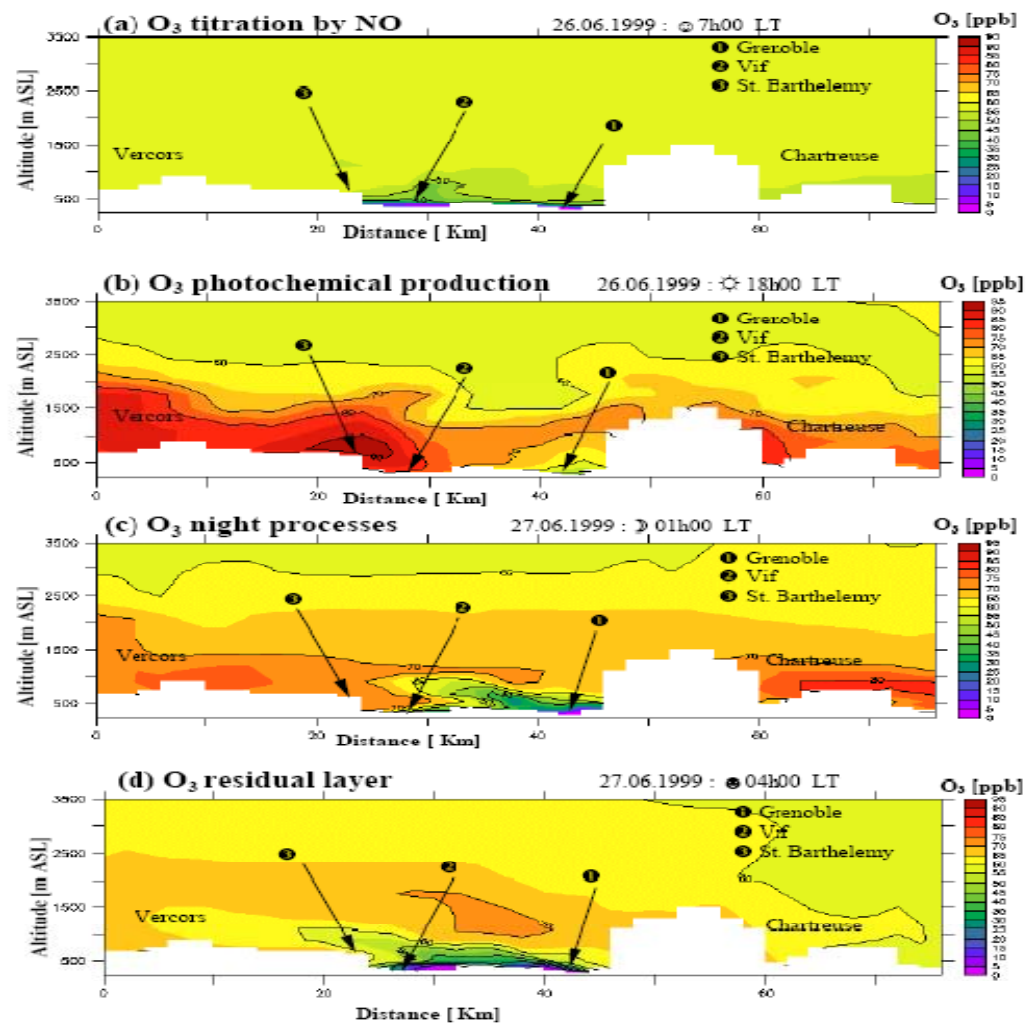
O. Couach et al., 2003 (Atmos.Chem.Phys. 3, 549-562)

Fig. 10. Simulated ozone dynamics in a south to north (Vif – Grenoble) 50 km transect from the ground to 3500 m ASL on the vertical dimension. The ozone NO titration in the morning (a), the ozone photochemical production (b), the night ozone processes (c) and the ozone residual layer formation (d) are represented here.